Diplomarbeit

Cardiac ryanodine receptor and regulation of nuclear Ca^{2+} in a mouse model of heart failure

eingereicht von

Clemens Reiter

zur Erlangung des akademischen Grades

Doktor(in) der gesamten Heilkunde

(Dr. med. univ.)

an der

Medizinischen Universität Graz

ausgeführt an der

Abteilung für Kardiologie

Universitätsklinik für Innere Medizin

unter der Anleitung von

Ass. Prof. Dr. Simon Sedej

und

Ljubojevic, Senka, PhD

Graz, 28. August 2015

Eidesstattliche Erklärung

Ich erkläre ehrenwörtlich, dass ich die vorliegende Arbeit selbstständig und ohne fremde Hilfe verfasst habe, andere als die angegebenen Quellen nicht verwendet habe und die den benutzten Quellen wörtlich oder inhaltlich entnommenen Stellen als solche kenntlich gemacht habe.

Graz, 28. August 2015 *Clemens Reiter, eh.*

Danksagungen

Ich möchte mich an dieser Stelle ganz herzlich bei meinem Betreuer Ass. Prof. PD Dr. Simon Sedej für die vielen wertvollen Ratschläge, Anregungen und Diskussionen bedanken. Durch ihn und seiner Aufgeschlossenheit neuen Ideen und Entwicklungen sowohl in der Medizin als auch der präklinischen Forschung gegenüber, konnte ich mich im Rahmen meiner Diplomarbeit mit dem faszinierenden Gebiet der Herzinsuffizienz beschäftigen.

Bedanken möchte ich mich auch bei Senka Ljubojevic, PhD für zahlreiche anregende Diskussionen im Zusammenhang mit Teilaspekten der vorliegenden Arbeit, bei Snjezana Radulovic, MSc. für ihre Hilfe im Labor sowie bei MMag. DDr Martin Kapl für seine Unterstützung bei der statistischen Auswertung.

Weiters gilt mein Dank dem gesamten Team der Forschungsgruppe Kardiologie der Universitätsklinik für Innere Medizin der Medizinischen Universität Graz für das anregende und freundliche Arbeitsklima.

Schlussendlich gilt mein ganz besonderer Dank meiner Freundin Alexandra Rieger, BSc für ihre Unterstützung und für ihr Verständnis dafür, dass ich viele Nächte und Wochenenden im Labor anstatt bei ihr zu Hause verbracht habe. Auch meinen Eltern, DI Dr. Ursula und DI Dr. Gert Reiter, die mir während meiner gesamten Studienzeit mit Ratschlägen zur Seite gestanden sind, möchte ich von ganzem Herzen aus danken.

Zusammenfassung

Veränderungen des Ca^{2+}-Haushalts im Zellkern finden bereits in der Frühphase der Herzumbauprozesse (z. B. Hypertrophie) und Herzinsuffizienz statt. Eine Fehlfunktion des kardialen Ryanodin-Rezeptors Typ 2 (intrazellulärer Kalziumkanal, RyR2) führt zu veränderter intrazellulären Ca^{2+}-Freisetzung, gestörter Ca^{2+}-Regulation im Zytoplasma und zu einem beschleunigten Herzmuskelumbau. Es ist jedoch nicht geklärt, ob die Fehlfunktion des RyR2 zu einer Veränderung der Ca^{2+}-Regulation im Zellkern unter Drucklast führt.

$RyR2^{R4496C+/-}$- („gain-of-function“ Mutation) und Wildtyp- (WT) Mäuse wurden transversale Aortenkonstriktion (TAC) unterzogen um die Drucklast aufs Herz zu erhöhen und Hypertrophie zu induzieren. Als Kontrolle wurden Mäuse einer Sham-Operation (Scheinoperation, Kontrolle) ohne Aortenkonstriktion unterzogen. Nach sieben Tagen wurden die ventrikuläre Herzmuskelzellen isoliert und mit 8 µmol/L Fluo-4/AM (Ca^{2+}-Farbstoff) beladen. Amplitude und Kinetik der Ca^{2+}-Transienten im Zytoplasma und Nukleus wurden während elektrischen Feldstimulation (1 Hz) mit einem Konfokalmikroskop im Line-Scan-Modus gemessen.

Amplitude und Kinetik von zytoplasmatischen und nukleären Ca^{2+}-Transienten von Herzmuskelzellen Sham-operierter Mäusen zeigten ein ähnliches Verhalten. Eine Woche nach TAC-Operation waren die zytoplasmatische Ca^{2+}-Transienten Amplituden von WT-Zellen jedoch erhöht, während die Amplitude und Kinetik der Ca^{2+}-Transienten im Zellkern nicht unterschiedlich waren. Im Gegensatz dazu kam es in $RyR2^{R4496C+/-}$-TAC-Zellen zu einer signifikanten Abnahme der Amplitude von zytoplasmatischen und nukleären Ca^{2+}-Transienten und einer langsameren Ca^{2+} Kinetik („time-to-peak“ und Ca^{2+} Abnahme) der nukleären Ca^{2+}-Transienten. Die Kombination von kongenitaler und erworbener RyR2-Fehlfunktion erhöht die Dauer von Ca^{2+}-Transienten und verringert ihre Amplitude in $RyR2^{R4496C+/-}$-TAC Herzmuskelzellen nach Drucklast. Diese Ergebnisse weisen darauf hin, dass es durch RyR2 verursachte Störung des Ca^{2+}-Haushalts zu Veränderungen der Gentranskription kommen könnte. Dies könnte in weiterer Folge den Herzmuskelumbau und die Genese der Herzinsuffizienz begünstigen.

Abstract

Early alterations of nuclear Ca^{2+} handling are associated with myocardial remodeling (e.g hypertrophy) and the development of heart failure. Defective intracellular Ca^{2+} release channel (ryanodine receptor type 2, RyR2) function disturbs cytosolic Ca^{2+} homeostasis and promotes myocardial remodeling. However, it remains elusive whether RyR2 dysfunction has an impact on the regulation of nuclear Ca^{2+} handling in response to pressure overload.

$RyR2^{R4496C+/-}$ (gain-of-function mutation) adult mice and their wild type (WT) littermates underwent Sham surgery (control) or transverse aortic constriction (TAC) to induce pressure overload. Ventricular cardiomyocytes were isolated seven days after surgery and loaded with 8 μmol/L Fluo-4/AM (Ca^{2+}-sensitive dye). Amplitudes and kinetics of Ca^{2+} transients in the cytoplasm and nucleus were monitored in electrically field-stimulated cardiac myocytes (at 1Hz) using confocal microscopy (line-scan mode).

Cardiomyocytes from Sham-operated mice showed similar cytoplasmic and nucleoplasmic Ca^{2+} transient amplitudes and kinetics. However, after 1 week of TAC the peak cytoplasmic Ca^{2+} transient amplitude was increased in WT cells, but nucleoplasmic Ca^{2+} transient amplitude and kinetics were normal. In contrast, $RyR2^{R4496C+/-}$-TAC cells had significantly smaller cytoplasmic and nucleoplasmic Ca^{2+} transient amplitudes as well as slower kinetics (time-to-peak and decay time) of nucleoplasmic Ca^{2+} transients.

The combination of acquired and congenital RyR2 dysfunction prolongs nuclear Ca^{2+} transients and reduces their amplitude in $RyR2^{R4496C+/-}$ hearts after pressure overload. These results suggest that RyR2-mediated Ca^{2+} changes in the nucleus may underlie altered gene transcription and promote cardiac remodeling.

Table of contents

Abbreviations

Ca^{2+}	Calcium
CaM	Calmodulin
CaMKII	Ca^{2+}/calmodulin-dependent protein kinase II
CICR	Ca^{2+}-induced Ca^{2+} release
CRU	Calcium release unit
CSQ	Calsequestrin
HDAC	Histone deacetylase
IP_3	Inositol-1,4,5-trisphosphate
IP_3R	Inositol-1,4,5-trisphosphate receptors
LTCC	L-type Ca^{2+} channels
NCX	Na^+/Ca^{2+} exchanger
NE	Nuclear envelope
NFAT	Nuclear factor of activated T-cells
NPC	Nuclear pore complexes
PKA	Protein kinase A
PLB	Phospholamban
PP1	Protein phosphatase 1
PP2	Protein phosphatase 2
RT50	Half maximum relaxation time
RT90	90% relaxation time (relaxation time to 90% of peak)
RyR2	Ryanodine receptor type 2
SERCA	Sarcoplasmic reticulum Ca^{2+}-ATPase
SR	Sarcoplasmic reticulum
TAC	Transverse aortic constriction
TTP	Time-to-peak
WT	Wild type

List of Figures

List of Tables

1 Introduction

1.1 Ca^{2+} is an ubiquitous second messenger

Calcium ion (Ca^{2+}) is the simplest and most versatile intracellular second messenger responsible for a variety of cellular functions. In cardiomyocytes, for example, Ca^{2+} regulates contraction (excitation-contraction coupling in the cytoplasm) and gene expression (excitation-transcription coupling in the nucleus), whereas Ca^{2+} overload can cause cell death [Bers 2008]. Altered intracellular Ca^{2+} homeostasis has emerged as a central pathophysiological mechanism in hypertrophy and heart failure. It is largely unknown what mechanisms cells use to decode changes in Ca^{2+} signals and how Ca^{2+} changes in subcellular compartments (e.g. nucleus) are regulated. However, different spatial and temporal properties of Ca^{2+} signals (i.e. amplitude, frequency, concentration and kinetics) may carry the information encoding different cellular actions [Bootman et al., 2001].

1.2 The role of Ca^{2+} in excitation-contraction coupling

In cardiomyocytes an action potential (excitation) triggers a transient rise of intracellular (global) Ca^{2+}, causing contraction. Afterwards, Ca^{2+} is removed from the cytosol; therefore, ending contraction and leading to relaxation. This strictly regulated cyclical process of Ca^{2+} increase and decrease is essential for Ca^{2+} homeostasis in the heart [Bers 2002].

1.2.1 Intracellular Ca^{2+} homeostasis

At the beginning of each heartbeat ventricular cardiomyocytes are depolarized by the activation of voltage-gated sodium channels and L-type Ca^{2+} channels (LTCC). Ca^{2+} influx through the LTCC increases local Ca^{2+} concentration up to 10-20 µmol within less than a millisecond [Bers 2008]. This in turn activates and opens ryanodine receptors type 2 (RyR2) that are localized on the sarcoplasmic reticulum (SR) [Fabiato 1983]. Ca^{2+} stored in the SR is massively released into the cytoplasm along its gradient (Figure 1) and increases the cytosolic Ca^{2+} concentration by a factor of 20 to 200-400 µmol [Bers 2008]. This process is called Ca^{2+}-induced Ca^{2+} release (CICR) [Fabiato 1983].

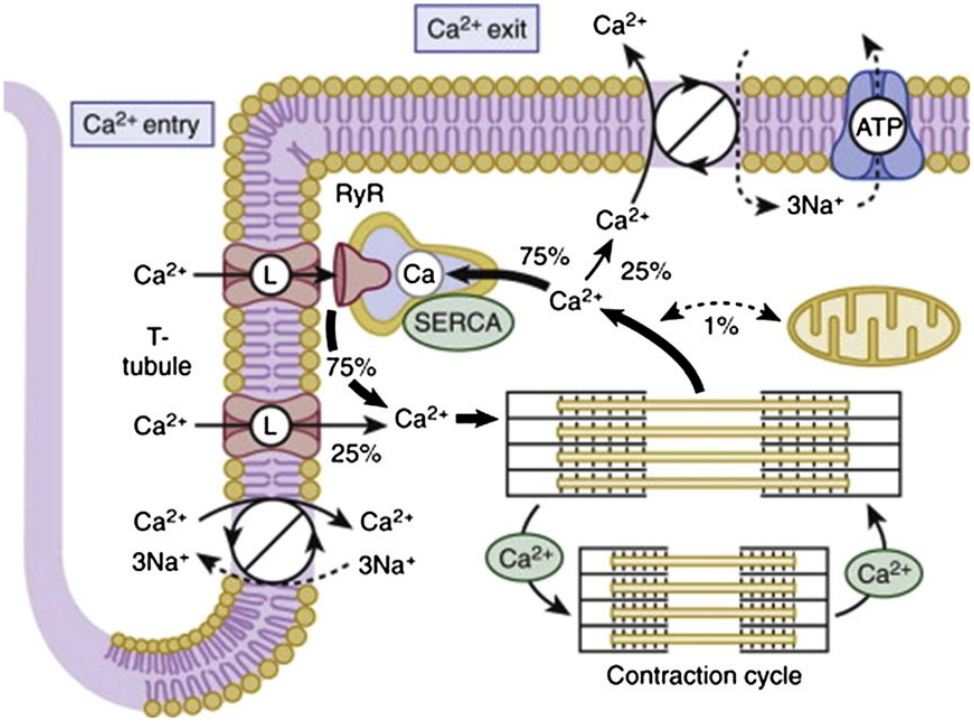

Figure 1: Calcium homeostasis in cardiac myocytes

Ca^{2+} entry via the voltage-gated L-type Ca^{2+} channels triggers Ca^{2+}-induced Ca^{2+} release, which is characterized by a massive Ca^{2+} release from the SR via RyR2 during the systole. Free Ca^{2+} then binds to cardiac myofibrils and activates contraction. For relaxation to occur, Ca^{2+} must be removed from the cytosol. Sarcoplasmic reticulum Ca^{2+}-ATPase (SERCA) (Ca^{2+} reuptake into the SR) and Na^{+}/Ca^{2+}- exchanger (Ca^{2+} transport out of the cell) are responsible for this process. Reprinted from [Braunwald 2013].

The increase of cytosolic Ca^{2+} concentration due to CICR initiates contraction of cardiomyocytes by binding of Ca^{2+} to the myofilaments (e.g. troponin C). This allows a subsequent binding of myosin to actin and the cyclic formation of cross-bridges, which generate force by the hydrolysis of ATP [Goody and Holmes 1982, Bers 2002].

For relaxation to occur, Ca^{2+} must be removed from the cytoplasm. The most important Ca^{2+} removal mechanisms are energy-dependent sarcoplasmic reticulum Ca^{2+}-ATPase 2a (SERCA2a) and Na^{+}/Ca^{2+}-exchanger (NCX) (Figure 1) [Braunwald 2013]. The relative contribution of respective mechanisms varies between species. In humans, about 70% of Ca^{2+} is removed by SERCA2a and 25% by NCX, whereas in rodents (e.g. mice and rats) about 90% of Ca^{2+} is retaken into the SR and only 5% is eliminated through the trans-sarcolemmal movement of Ca^{2+} mediated by NCX and plasma membrane Ca^{2+}-ATPase [Bers 2008]. SERCA2a is regulated by phospholamban (PLB). Phosphorylated PLB is inactive and exists in the cytosol as pentamer. When dephosphorylated, PLB depolymerizes

and binds to SERCA2a inhibiting its activity. SERCA2a's activity is regulated by protein kinase A (PKA) and/or Ca^{2+}/calmodulin-dependent protein kinase II (CaMKII), resulting in increased SR Ca^{2+} content (positive inotropic effect) and faster Ca^{2+} elimination from the cytosol (positive lusitropic effect) [Fearnley et al., 2011].

The second major Ca^{2+} removal mechanism is via an electrogenic antiporter – NCX. [Shigekawa and Iwamoto 2001]. During the diastole and most of the systole, NCX uses the energy stored in the electrochemical gradient across the plasma membrane to exchange 1 intracellular Ca^{2+} against 3 extracellular Na^{+}, thereby generating a depolarizing inward current [Bers 2008].

The remaining Ca^{2+} is removed by the plasma membrane Ca^{2+}-ATPase and the mitochondrial Ca^{2+} uniporter [Fernley et al., 2011].

1.2.2 Membrane structures and Ca^{2+}-dependent proteins involved in the SR Ca^{2+} release

Intracellular Ca^{2+} concentration is increased via two major pathways: (1) Ca^{2+} enters the cell via LTCC and (2) Ca^{2+} is released through RyR2 from the SR, which is a major cellular Ca^{2+} storage compartment and rich in RyR2. Specialized domains of the SR interact with domains of the sarcolemma, where LTCC are located. RyR2s form Ca^{2+} release units (CRUs) of different geometries, which are termed peripheral couplings (junctions between sarcolemma and SR), dyads (SR interacts with T-tubules), or corbular SR (SR is not associated with the sarcolemma). CRUs are constituted of 5 components: LTCC, RyR2, triadin, junctin, and the intra-SR Ca^{2+}-binding protein calsequestrin [Franzini-Armstrong et al., 1999, Franzini-Armstrong et al., 2005]. T-tubules are geometrically complex invaginations of the sarcolemma, which allow rapid propagation of electric signals along the cell [Soeller and Cannell 1999]. The gap between the SR and the T-tubule/sarcolemma, where CICR takes place is termed diadic cleft [Langer and Peskoff 1996]. The number of RyR2s disposed per LTCC and diameters of the dyadic clefts is highly variable [Hayashi et al., 2009].

Cardiac RyR2 is an intracellular SR Ca^{2+} release channel [Otsu et al., 1990, Nakai et al., 1990], which has been named after its modulation by a plant alkaloid ryanodine [Pessah et al., 1985]. The cardiac RyR2 is a large protein of 4,969 amino acids with a molecular weight of about 564 kDa, existing as a tetramer [Otsu et al., 1990]. The channel consists of a

cytoplasmic and a transmembrane region (Figure 2) and forms a macromolecular complex with various other regulatory proteins. On its intra-SR (luminal) site, RyR2 interacts with junctin and triadin. On the cytosolic site, RyR2 interacts with numerous proteins, including calmodulin (CaM), CaMKII, FKBP, PKA, protein phosphatase 1 or 2 (PP1, PP2). These proteins modulate RyR2 function by altering the opening probability of the RyR2 through the de-/phosphorylation [Bers 2004].

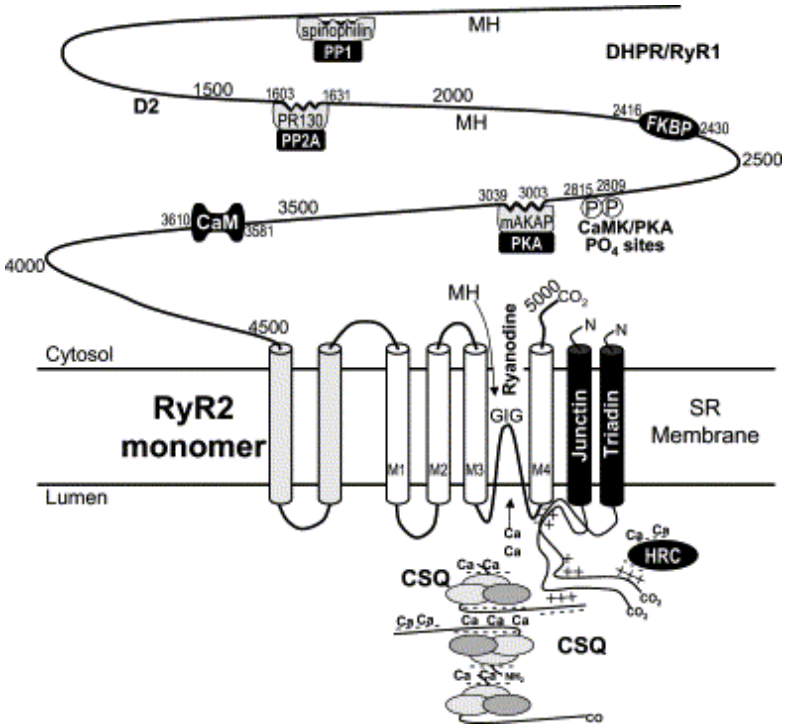

Figure 2: Structure of RyR2

SR domain with interaction sites for calsequestrin (CSQ), junctin and triadin, and the larger cytosolic domain with interaction sites for various proteins like Ca^{2+}/calmodulin-dependent kinase II (CaMKII), protein kinase A (PKA), protein phosphatase 1 and 2 (PP1, PP2, respectively) or calmodulin (CaM). Reprinted from [Bers 2004].

1.2.3 Dysregulation of cytosolic Ca^{2+} homeostasis

As described above, normal Ca^{2+} homeostasis is a key determinant of normal cardiac function. Contractile dysfunction in heart failure is caused by abnormal cellular Ca^{2+} handling and changes in contractile proteins [Piacentino et al., 2003]. Cardiomyocytes from failing hearts display altered intracellular Ca^{2+} homeostasis by exhibiting increased baseline (diastolic) Ca^{2+} concentration, decreased Ca^{2+} amplitudes and slower Ca^{2+} removal,

contributing to disrupted myocardial contractility and relaxation [Beuckelmann et al., 1992, Hasenfuss and Pieske 2002, Piacentino et al., 2003, Luo and Anderson 2013]. Various structural and functional changes, such as (i) altered organization of the T-tubule system, (ii) increased SR Ca^{2+} release, (iii) reduced expression and activity of SERCA2a and (iv) increased expression of NCX contribute to altered cytoplasmic Ca^{2+} homeostasis (Figure 3).

Normal (regular) T-tubule structure becomes irregular in the progression to heart failure [Lyon et al., 2009]. When T-tubules are lost, RyR2 can become orphaned from LTCC [Wei et al., 2010]. CICR is compromised due to weaker LTCC-RyR2 coupling, which reduces Ca^{2+} release in close proximity of the orphaned RyR2. Thus, Ca^{2+} from remote areas diffuses to these orphaned RyR2, causing delayed opening, ineffective contraction and arrhythmias [Song et al., 2006, Luo and Anderson 2013]. Furthermore, a given increase in Ca^{2+} through LTCC triggers lower SR Ca^{2+} release through RyR2 than in normal cardiomyocytes [Gomez et al., 1997].

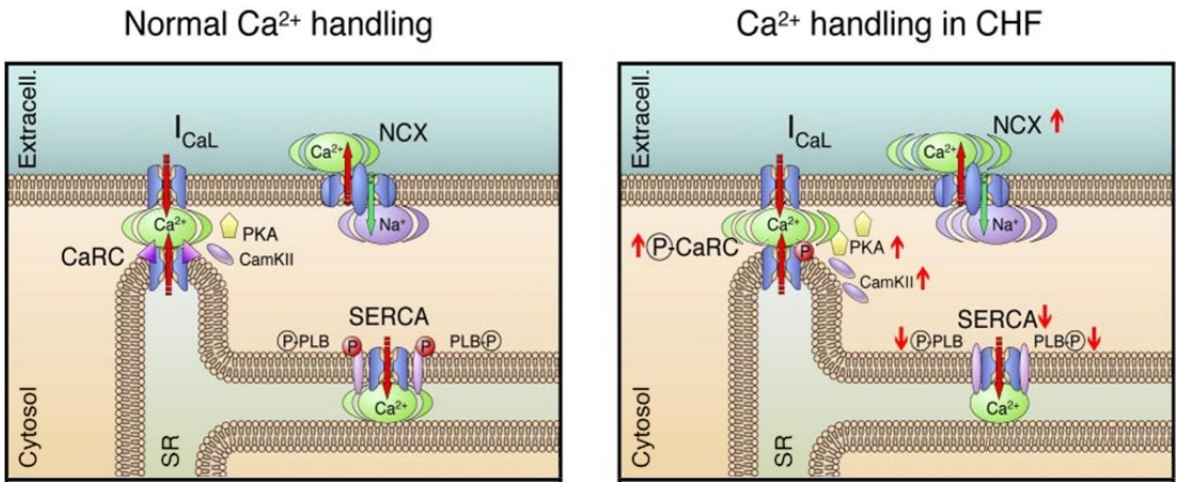

Figure 3: Alterations of cytosolic Ca^{2+} handling in chronic heart failure

Sustained (chronic) phosphorylation via PKA/CaMKII increases the probability of the RyR2 opening which leads to spontaneous (diastolic) SR Ca^{2+} leak. SERCA2a activity is decreased by reduced phosphorylation of phospholamban (PLB). Increased intracellular Ca^{2+} concentration increases the activity of NCX in forward mode (Ca^{2+} extrusion). Adapted from [Nattel et al., 2007].

Elevated RyR2 phosphorylation by PKA and/or CaMKII during beta-adrenergic stimulation leads to increased diastolic (spontaneous) SR Ca^{2+} release (also called SR Ca^{2+} leak) [Ai et al., 2005, Morimoto et al., 2009]. Furthermore, depletion of phosphatases in failing

cardiomyocytes decreases dephosphorylation of RyR2 [Reiken et al., 2002] and other proteins [Neumann et al., 1997].

Reduced expression and activity of SERCA2a (due to reduced PLB phosphorylation) in failing cardiomyocytes contributes to decreased SR Ca^{2+} uptake [Meyer et al., 1995].

In heart failure, the relative amount of Ca^{2+} removed by NCX is increased, probably because of depressed SR Ca^{2+} uptake and increased NCX expression [Hasenfuss and Pieske 2002]. Since Na^{+} concentration is also elevated in heart failure, NCX can change the direction of ion transport, leading to prolonged Ca^{2+} entry during the action potential and Ca^{2+} overload at higher frequencies [Pieske et al., 2002]. The combination of decreased SERCA2a and increased NCX lowers the SR Ca^{2+} content and, at the same time, facilitates trans-sarcolemmal Ca^{2+} extrusion, resulting in impaired contraction. [Hobai and O'Rourke 2001]

1.2.4 From hypertrophy to heart failure - the role of RyR2 and Ca^{2+}

Altered intracellular Ca^{2+} homeostasis has emerged as a central pathophysiological mechanism in hypertrophy and heart failure, because reduced systolic increases in intracellular Ca^{2+} concentration contribute to depressed ventricular contractile function [Hasenfuss and Pieske 2002]. On the other hand, diastolic levels of cytosolic Ca^{2+} concentration during heart failure are increased. Beat-to-beat changes in Ca^{2+} concentration underlying contraction and relaxation of the heart muscle constitute Ca^{2+} transients, which are generated by transient SR Ca^{2+} release via RyR2. In addition to rhythmic changes in intracellular Ca^{2+} concentration, Ca^{2+}-dependent signaling has also been assigned a central role in hypertrophy [Bers 2008]. Increased intracellular Ca^{2+} concentration regulates maladaptive remodeling at the cellular as well as molecular level by Ca^{2+}-mediated activation of hypertrophic signaling pathways (excitation-transcription coupling) [Domínguez-Rodríguez 2012]. Gene transcription regulation is essentially mediated by phosphorylation or by alterations in subcellular localization of transcription factors. Recent studies pointed out that defective regulation of the RyR2 is associated with increased spontaneous Ca^{2+} release [Fischer 2013], which leads to contractile dysfunction and triggers fatal arrhythmias [Bers 2008]. Major causes of death in advanced heart failure are sudden cardiac death and pump failure [Carson et al., 2005]. Importantly, the combination of congenital RyR2 abnormalities and pressure overload accelerate cardiac structural and functional remodeling in mice carrying a RyR2 gain-of-function mutation [van Oort et al.,

2010, Sedej et al., 2014]. These transgenic mice exhibit heart failure (HF) phenotypes characterized by eccentric hypertrophy, ventricular dilatation and increased fibrosis under pressure overload. In line with this, cardiac myocytes carrying a RyR2 gain-of-function mutation have increased SR Ca^{2+} leak associated with altered cytoplasmic Ca^{2+} handling [Sedej et al., 2014]. Other underlying mechanisms (besides "leaky" RyR2) contributing to altered Ca^{2+} handling and thus heart failure include: defective sequestration of Ca^{2+} due to decreased expression and phosphorylation of the PLB-regulated Ca^{2+} ATPase (SERCA2a) and increased expression of sarcolemmal NCX [Bers 2008]. Increased NCX activity causes SR Ca^{2+} depletion and Ca^{2+} elimination from cardiomyocytes.

Evidence suggests that intracellular Ca^{2+} signaling is different in hypertrophy (with increased Ca^{2+} transients) and heart failure [Bers 2008]. This may lead to Ca^{2+} overload and increased SR Ca^{2+} leak, which might contribute to the progression of heart failure. Furthermore, a recent study showed that disturbances of nuclear Ca^{2+} handling occur earlier than changes in cytosolic Ca^{2+} handling and precede the development of cardiac dysfunction [Ljubojevic et al., 2014]. Collectively, it appears that increased SR Ca^{2+} leak is regulated differently in hypertrophy and heart failure and it may contribute to disturbances of nuclear Ca^{2+} handling and thus, gene expression (i.e. excitation-transcription coupling).

1.3 The role of Ca^{2+} in excitation-transcription coupling

1.3.1 Nuclear Ca^{2+} homeostasis

The nuclear envelope (NE) is the major nuclear Ca^{2+} store and consists of an inner and outer nuclear membrane. The outer nuclear membrane is continuous with the SR [Wu and Bers 2006]. The nuclear envelope is interrupted by nuclear pore complexes (NPCs) that allow diffusion of Ca^{2+} [Lee et al., 1998], and therefore, contribute to a passive component of nuclear Ca^{2+} transients [Ljubojevic and Bers 2015]. It has been suggested that NPCs can modulate the diffusion of Ca^{2+} into the nucleus [Bootman et al., 2009]. However, the underlying mechanisms are not fully understood.

In addition to the passive diffusion of Ca^{2+} into the nucleus, the activation of inositol-1,4,5-trisphosphate receptors (IP_3R) by inositol-1,4,5-trisphosphate (IP_3), actively increases nuclear Ca^{2+} concentration and shapes nuclear Ca^{2+} signals [Kockskämper et al., 2008]. Rhythmic (beat-to-beat) Ca^{2+} rise and decay in the nucleoplasm (nuclear Ca^{2+} transients) have smaller amplitudes and slower kinetics than cytoplasmic Ca^{2+} transients [Ljubojevic et

al., 2011]. The removal of nuclear Ca^{2+} is slower due to the lack of Ca^{2+}-ATPase on the inner nuclear membrane. Therefore, Ca^{2+} must diffuse out of the nucleus [Bootmann et al., 2009]. However, at high stimulation frequencies this slow removal can lead to diastolic Ca^{2+} accumulation in the nucleus [Ljubojevic et al., 2011].

A recent study demonstrated a close spatial relationship between the NE, T-tubules and RyR2 containing perinuclear dyads in mouse ventricular cardiac myocytes (Figure 4) [Escobar et al., 2011], suggesting the existence of perinuclear Ca^{2+} microdomains. Under conditions of enhanced IP_3 signaling (i.e. heart failure) [Signore et al., 2013], Ca^{2+} release from RyR2 containing perinuclear dyads might sum up with Ca^{2+} released by IP_3. This could affect the amplitude and/or the kinetics of peri/nuclear Ca^{2+} transients.

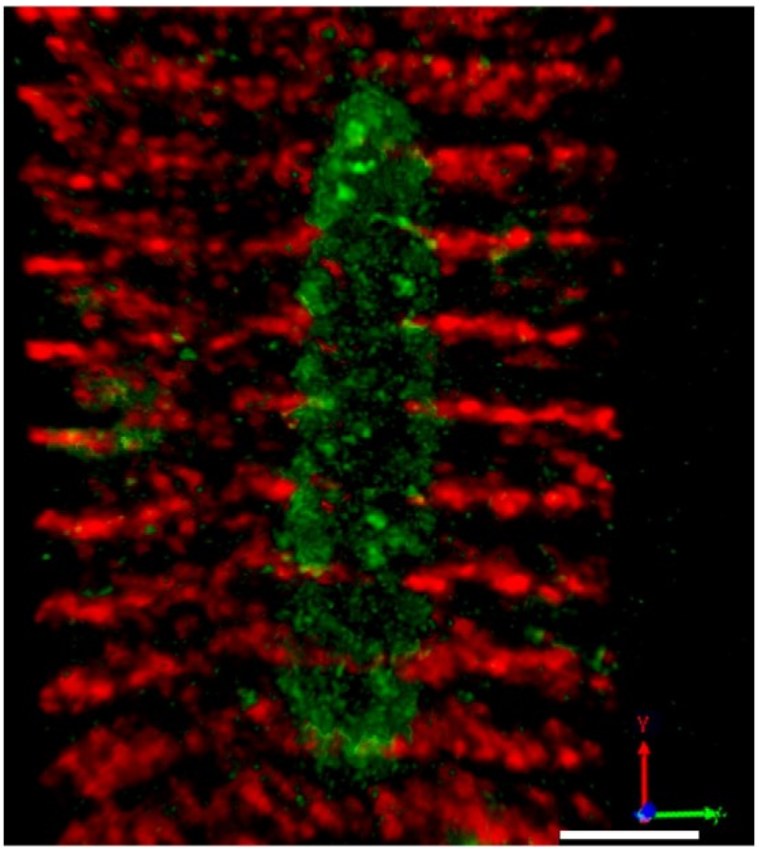

Figure 4: Colocalization of RyR and IP_3R

Around the nucleus RyR2 (labeled red) and IP_3R (labeled green) come into close contact and form local Ca^{2+} microdomains. Reprinted from [Escobar et al., 2011].

1.3.2 Alterations of nuclear Ca^{2+} homeostasis in failing cardiomyocytes

In hypertrophied and failing cardiomyocytes, there are a number of structural and functional changes of the NE: (1) decreased number of nuclear invaginations, (2) enlarged nuclei, (3) decreased SERCA2a expression, (4) increased IP_3R density and (5) reduced density of RyR2 in the perinuclear space (Figure 5). This suggests that compromised cytoplasmic-nuclear passive and active interactions play an important role in altered nuclear Ca^{2+} homeostasis. Small nuclear Ca^{2+} amplitudes, slow removal and elevation of diastolic nuclear Ca^{2+} are typical alterations of nuclear Ca^{2+} homeostasis in failing cardiomyocytes [Ljubojevic et al., 2014]. Furthermore, altered NPC composition in failing cardiomyocytes may alter nucleocytoplasmic transport and therefore, additionally deteriorate nuclear Ca^{2+} homeostasis [Tarazon et al., 2012].

Increased IP_3 signaling stimulates Ca^{2+} release from the NE (Figure 5) and the activation of many Ca^{2+}-dependent hypertrophic signaling pathways, such as calcineurin-NFAT (nuclear factor of activated T-cells) and CaMKII-HDAC (histone deacetylase), thereby influencing gene transcription [Wu et al., 2006].

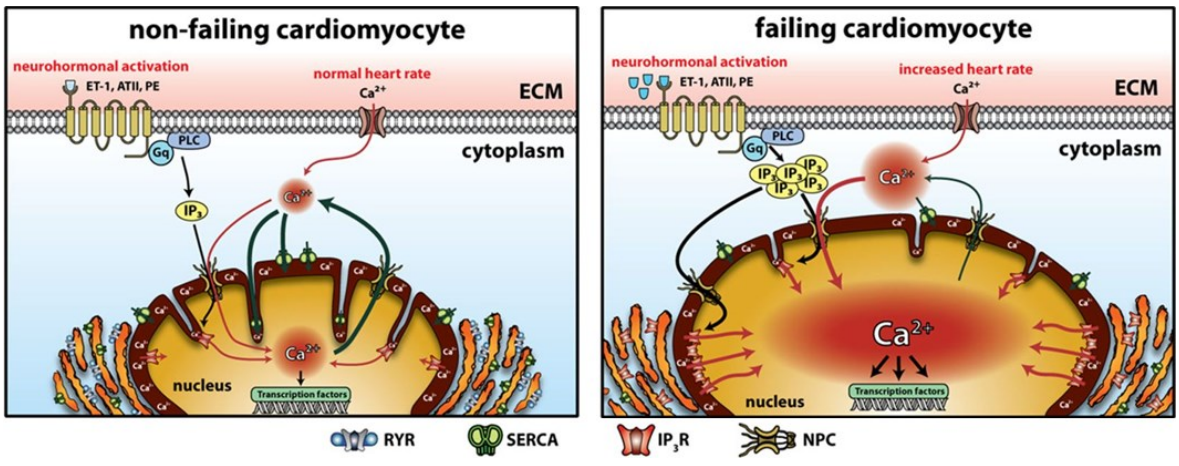

Figure 5: Alteration of nuclear Ca^{2+} in heart failure

The nucleus is enlarged in a failing cardiomyocyte. Enhanced stimulation of G-protein coupled receptors by different hormones (e.g. endothelin-1, angiotensin-II) increase the levels of IP_3. IP_3 diffuses to the nucleus and activates IP_3R, leading to increased Ca^{2+} release in the nucleus. Since Ca^{2+} has to diffuse out of the nucleus in order to be retaken by the NE/SR, Ca^{2+} is especially increased at higher pacing frequencies. The SR is in close proximity of the NE and thus, forms a functional compartment with which it might affect nuclear Ca^{2+} by enhanced diastolic Ca^{2+} release. Reprinted from [Ljubojevic et al., 2014].

1.4 Work that led to this study and hypothesis

The combination of pressure overload and gain-of-function mutation of RyR2 causes alterations in cytoplasmic Ca^{2+} handling and accelerates progression from hypertrophy to heart failure [Sedej et al., 2014]. At the same time, changes in nuclear Ca^{2+} handling are an early event of cardiac remodeling in the development of heart failure [Ljubojevic et al., 2014]. Given that the SR and the NE come into close proximity thereby forming a functional compartment [Wu and Bers 2006], it seems plausible that dysfunctional RyR2-mediated Ca^{2+} release plays a role in the regulation of perinuclear and nuclear Ca^{2+}. In this work, the hypothesis that the $RyR2^{4496C+/-}$ gain-of-function mutation reduces peri-/nuclear Ca^{2+} amplitude and delays the kinetics of peri-/nuclear Ca^{2+} transients after pressure overload was tested.

2 Material and Methods

2.1 Mice

Experiments were performed on male and female heterozygous $RyR2^{R4496C+/-}$ (RyR) knock-in mice [Cerrone et al., 2005] and their wild type (WT) littermates (C57/B6 strain; N= 10 and 12 mice, respectively) at the age of 9-15 weeks. All animal procedures described below were approved by the Austrian government agencies (BMWFW-66.010/0075-WF/II/36/2014).

2.2 Transverse aortic constriction (TAC)

Minimally invasive transverse aortic constriction (TAC) is an established experimental procedure to induce pressure overload and left ventricular hypertrophy in mice [Hu et al., 2003, Toischer et al., 2010, Muhlfeld et al., 2013].

Mice of 21±1 g (females) and 24±1 g (males) body weight were anesthetized with intraperitoneal administration of ketamine (80 mg/kg body weight) and xylazine (5 mg/kg body weight). Then self-ventilating mice underwent standardized a TAC procedure using a 27-gauge needle. A horizontal incision at the jugulum was used to visualize the aorta. The 27-gauge blunted needle was placed parallel to the transversal part of aorta and tied against the aorta (between the right innominate artery and the left common carotid artery) using a suture. After removal of the 27-gauge needle, the skin was closed. Mice were kept on a warming pad at 37°C until complete recovery from anaesthesia. A subgroup of mice underwent a sham procedure consisting of aortic exposure without ligation. All mice received analgesic Metamizol-Sodium (15 drops dissolved in 100 ml drinking water) for 1 week. All surgical procedures were performed by Dr. Simon Sedej, who was blinded to the genotype. For all experimental protocols similar numbers of males and females were used in each group to avoid potential gender-related bias.

2.3 Isolation of adult ventricular cardiomyocytes

One week after surgery, $RyR2^{R4496C+/-}$ and WT mice were anesthetized with isoflurane, weighed and administrated intraperitoneally 100 µl (50 I.U.) heparin solution (Table 1) to

prevent formation of blood clots during the cell isolation. After cervical dislocation, hearts were rapidly excised, weighed and placed into an ice-cold cannulation solution (Table 2).

Table 1: Heparin solution

Compound	Volume	Final concentration (I.U./ml)
5000 I.U. Heparin	0.1 ml	500
0.9% NaCl solution	0.9 ml	

Table 2: Cannulation solution

Compound	Quantity	Final concentration (mmol)
Perfusion buffer solution[#]	150 ml	
$CaCl_2$ (1M stock solution)	150 µl	1

[#] for composition see Table 3

Table 3: Perfusion stock solution

Substance	Molecular weight (g/mol)	Concentration (mmol)
NaCl	58.44	135
KCl	75.56	4.7
KH_2PO_4	136.1	0.6
Na_2HPO_4 *$7H_20$	268.07	0.6
$MgSO_4$ *$7H_20$	246.5	1.2
HEPES	238.3	10
Taurine	125.1	30

The aorta was rapidly cannulated to allow optimal retrograde perfusion of the myocardium via the coronary vessels. Correct cannulation was checked by a visual inspection of coronary vessels, which were free of blood after the perfusion with the cannulation solution (Figures 6-8).

Figure 6: Cannulation setup

a) Box with ice, b) Petri dish with cannulation solution, c) Stereomicroscope, d) Light source, e) Syringe with cannulation solution

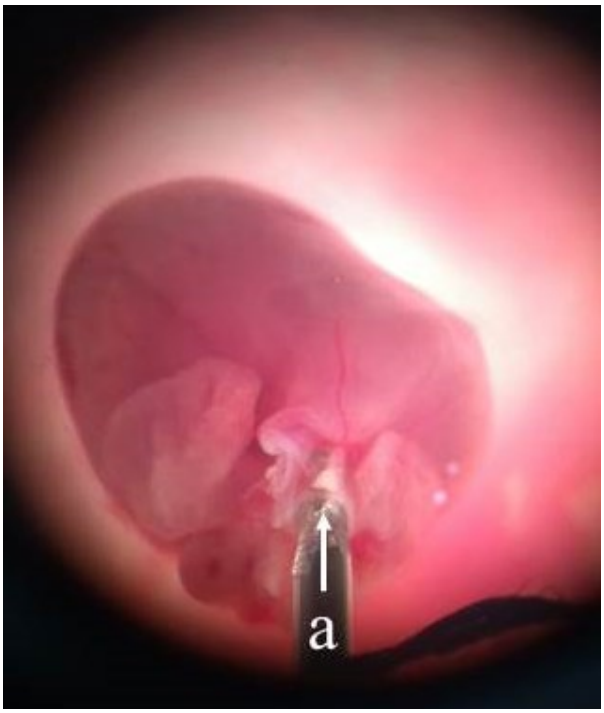

Figure 7: Cannulated aorta

The tip of the syringe is placed in the aorta (a) for retrograde perfusion through coronary vessels. Magnification: 120x.

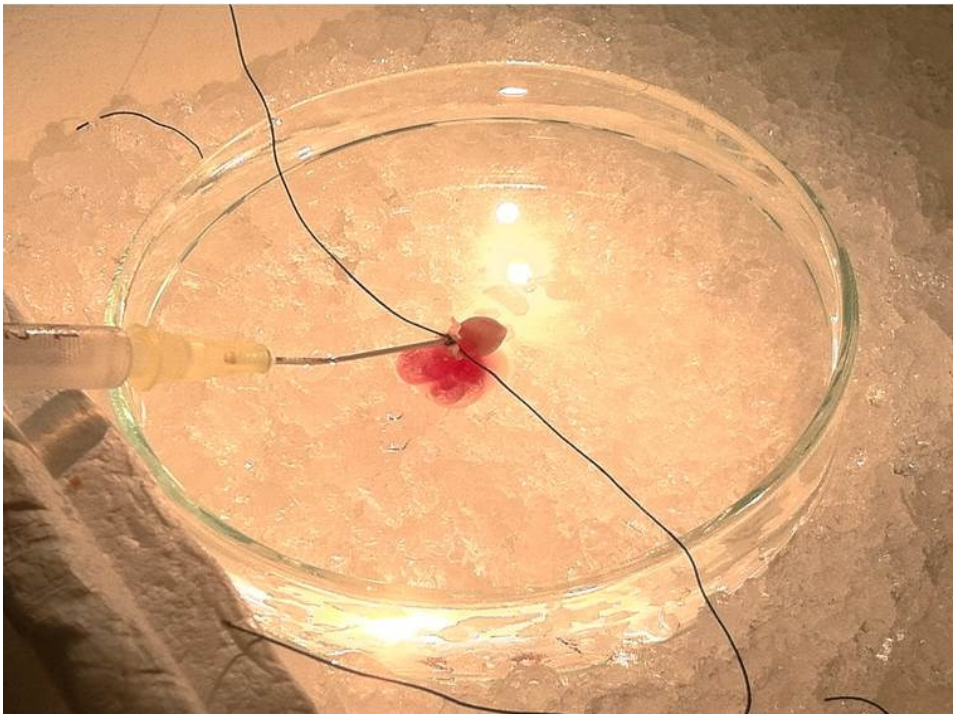

Figure 8: Perfusion of the cannulated heart

The heart with the aorta tied to the syringe is perfused with an ice-cold cannulation solution.

The heart was mounted on the Langendorff system, which is used for the isolation of cardiac myocytes. The Langendorff system consists of two glass beakers filled with perfusion solution and digestion solution, tubing, bubble trap and a peristaltic pump to provide a fixed flow rate (3 ml/min) to the heart (Figure 9). Langendorff system tubing is connected to a temperature-controlled water bath to maintain the temperature of solutions and beakers at 37°C, which is optimal for enzymatic reactions, and thus digestion. Ventricular myocytes were isolated using a liberase-based enzymatic digestion protocol [O'Connell et al., 2003, Sedej et al., 2010].

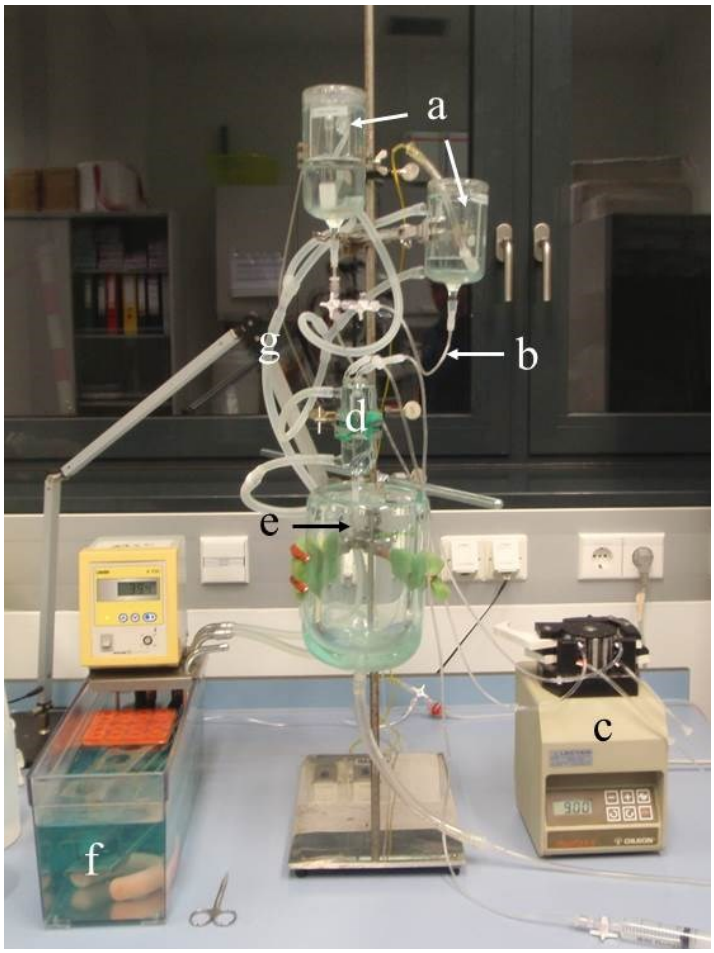

Figure 9: The Langendorff setup

(a) Water jacketed glass beakers for perfusion and digestion solution, (b) Perfusion tube, (c) Peristaltic perfusion pump, (d) Bubble trap, (e) Mounting site for cannula, (f) Water bath, (g) Water jacket tube.

The heart was first perfused with Ca^{2+}-free perfusion solution (Table 3 and Table 4) for 4 minutes followed by liberase/trypsin digestion solution (Table 5) for further 7 minutes.

Table 4: Perfusion solution

Compound	Quantity	Final concentration (mmol)
Perfusion stock solution[#]	333 ml	
2,3-Butanedione monoxime	337 mg	10
Glucose	600 mg	10

[#] for composition see Table 3

Table 5: Digestion solution

Compound	Quantity	Final concentration (mg/ml)
Perfusion solution (Table 4)	25 ml	
Liberase TM Research Grade[#]	300 µl	0.075
Trypsin x10 liquid[*]	111 µl	0.056

Digestion Enzymes: LiberaseTM (Roche, Switzerland) aliquots of 300 ml (~1.5 mg) and Trypsin (ThermoFisher Scientific) aliquots of 111 ml (10x; 0,05 mg/ml) were prepared and stored at -20°C.

Then the ventricles were cut off, put into a beaker with the stopping solution 1 (Table 6), and cut into small pieces.

Table 6: Stopping solution 1

Compound	Quantity	Final concentration
Perfusion solution (Table 4)	2.25 ml	
Bovine calf serum	0.25 ml	0.25 mg/ml
10 mmol $CaCl_2$	3.125 µl	12.5 µmol

Cells were dissociated by gently pipetting heart tissue using Pasteur pipettes with decreasing size openings (smaller diameters) to gradually increase mechanical stress. Cell suspension was filtered through a 300×300 µm mesh into a Falcon tube. The myocytes were allowed to sediment by gravity for 10 minutes. Cells formed a pellet (Figure 10) at the bottom of the 15 ml Falcon tube.

Figure 10: Formation of cell pellet

Isolated cardiomyocytes were allowed to sediment and form a pellet (a).

In order to reintroduce Ca^{2+} to the cells, which had been removed during isolation, it is necessary to slowly (stepwise) rise the extracellular Ca^{2+} level. The supernatant was removed and the cell pellet was re-suspended in the stopping solution 1 supplemented with 0.125 mmol Ca^{2+} (Table 7) for 10 min at room temperature. This step was repeated two times by removing the supernatant and adding the stopping solution 2 with increasing Ca^{2+} concentration, namely 0.25 mmol Ca^{2+} and 0.5 mmol Ca^{2+} (Table 7).

Table 7: Ca^{2+} solutions

0.125 mmol Ca^{2+} solution

Compound	Volume	Final concentration
Myocyte stopping solution 2[#]	8 ml	
100 mmol $CaCl_2$	10 µl	0.125 mmol

[#]see Table 8

0.25 mmol Ca^{2+} solution

Compound	Volume	Final concentration
Myocyte stopping solution 2[#]	4 ml	
100 mmol $CaCl_2$	10 µl	0.25 mmol

[#]see Table 8

0.5 mmol Ca^{2+} solution

Compound	Volume	Final concentration
Myocyte stopping solution 2[#]	8 ml	
100 mmol $CaCl_2$	40 µl	0.5 mmol

[#]see Table 8

Table 8: Stopping solution 2

Compound	Volume	Final concentration
Perfusion solution (Table 3)	19 ml	
Bovine calf serum	1 ml	0.125 mg/ml
10 mmol $CaCl_2$	25 µl	12.5 µmol

Ten minutes were allowed between the steps for cells to sediment. Thereafter cells were kept in normal Tyrode's solution 1 (Table 9). Only quiescent, Ca^{2+}-tolerant, rod-shaped, and

cross-striated myocytes were used for experiments within 4 hours after the isolation (Figure 11).

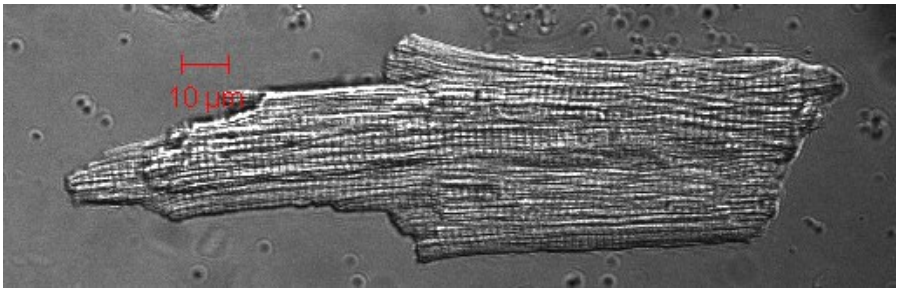

Figure 11: Transmission light microscopy image of an isolated ventricular cardiomyocyte
Cardiomyocytes are rod shaped and exhibit the cross-striations.

Table 9: Normal Tyrode's solution 1

Compound	Molecular weight (g/mol)	Concentration (mmol)
NaCl	58.44	136
KCl	75.56	5
$CaCl_2$ *$2H_20$	147.02	1
$MgCl_2$ *$6H_20$	203.3	1
HEPES	238.3	10
Glucose	180.2	10

All solutions were prepared prior to isolation, except the stock solutions which were stored for up to one week. Reagents were purchased from Sigma-Aldrich® (St. Louis, USA), unless otherwise stated. The adjustment of pH to 7.45 was done at room temperature.

2.4 Confocal Microscopy

The main advantage of confocal microscopy over conventional fluorescence microscopy is that only a chosen optical section of a specimen is scanned, whereas information of out-of-focus light is suppressed. Therefore, axial resolution, which cannot be resolved in conventional fluorescence microscopy, can be scanned [Shotton 1989].

The principle of a confocal laser fluorescence microscope is shown in Figure 12: A light source emits coherent light of the chosen wavelength. After passing the pinhole of the illuminating aperture, the light is reflected by a dichroic mirror and focused by the objective lens onto the specimen, and causes fluorescence by exciting a fluorescent dye. Emitted fluorescence light passes back through the dichroic mirror where it does not get reflected but is focused on the image aperture and detected by a photomultiplier, after passage of a pinhole. This pinhole blocks fluorescence light from above and below the focal plane, which therefore is not detected by the photomultiplier [Paddock 2000]. To minimize interference signals, additional filters at the light source and at the detector allow selection of passing wavelengths.

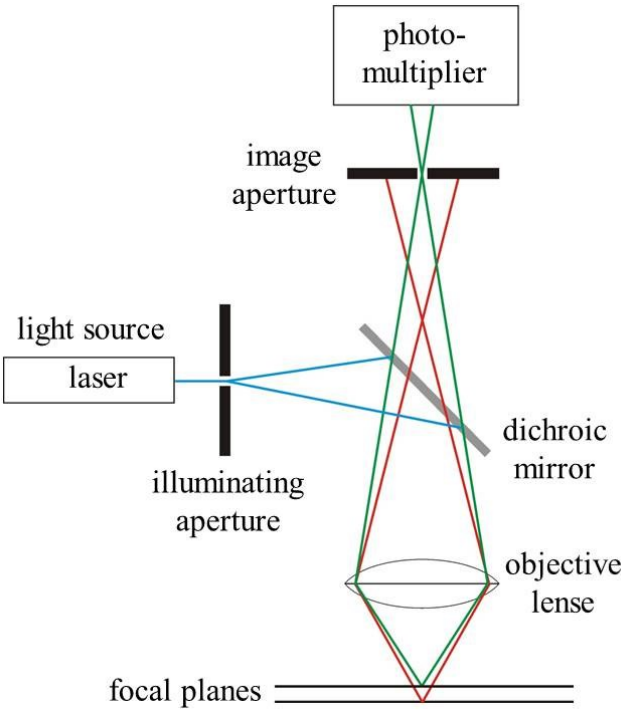

Figure 12: Illustration of the principle of laser confocal microscopy

As light source a laser was used (blue path). Two optical paths from different focal planes are shown, whereby fluorescence from the upper layer (green path) is able to pass the pinhole (called in-focus ray) and is recorded. The optical path (red) from the lower focal plane cannot pass the pinhole and therefore gets filtered out, called out-of-focus ray. Adapted from [Shotton 1989].

As signal is only gathered from the point of focus, one need to stepwise scan a layer to assemble the final image. This is done by moving the focus probe and scanning all the lines of the two dimensional raster [Shotton 1989, Paddock 2000].

Confocal $[Ca^{2+}]_i$ measurements were acquired at maximum line scan speed by a confocal microscope (LSM 510 Meta, Zeiss, Germany) equipped with a Zeiss Plan Neofluar 40x/1.3 DIC oil-immersion objective. Scanning was performed in unidirectional line scan mode: A chosen line was recorded repeatedly over time, and plotted as an image where the x-axis represents time, and the y-axis the scan line (Figure 13).

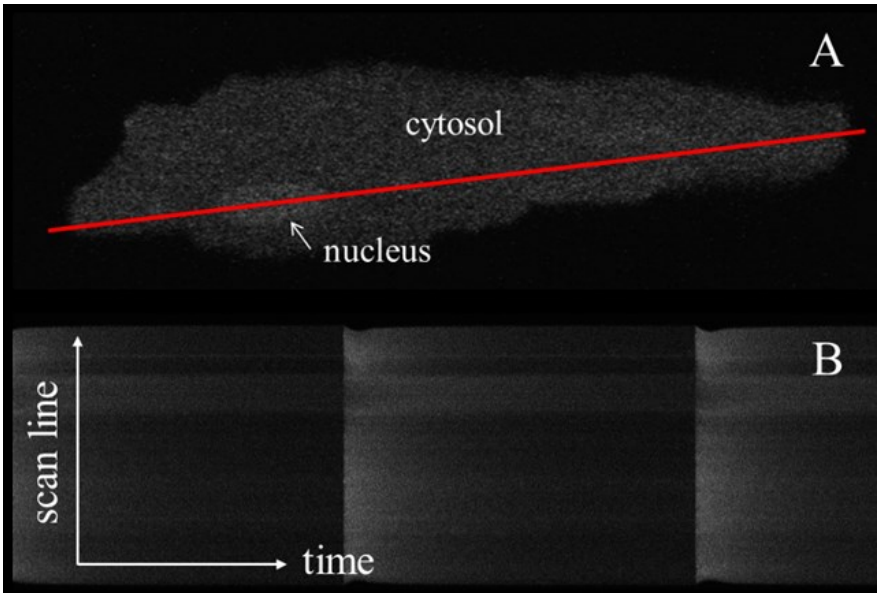

Figure 13: Illustration of the principle of line-scan mode

(A) Line is drawn along the longitudinal axis of a cardiomyocyte including the cytosol and nucleus and part of the background. (B) Original line-scan image, whereby x-axis represents time and y-axis represents the scan length. Increased brightness represents increased fluorescence intensity and thus, increased Ca^{2+} concentration.

Fluo-4/AM stock aliquots (Life Technologies®, Carlsbad, California) were prepared in a darkened room by dissolving 50 µg Fluo-4/AM (vial content) in 9 µl DMSO resulting in 5.06 mmol Fluo-4/AM. The aliquots were wrapped in an aluminum foil to protect from light and stored at -20°C. Cardiomyocytes were loaded with 8 µmol/L Fluo-4/AM and 0.42 mg/mL Pluronic® F-127 (20% solution in DMSO) dissolved in Tyrode's solution 1 (Table 9) for 45 min at room temperature. Myocytes were then plated on laminin-coated coverslips, washed with Normal Tyrode's solution 1 and at least 15 minutes were allowed for de-esterification of the dye.

Myocytes were placed on the stage of (the) confocal microscope, superfused with Normal Tyrode's solution 2 (Table 10) delivered by a gravity-driven and heated (35-37°C) superfusion pipette and field stimulated for 2 min at 1 Hz at room temperature to reach a steady-state. Fluo-4/AM was excited at 488 nm using an argon-ion laser and the emitted

light ≥505 nm was collected. Only rhythmically (1 Hz) contracting cells were selected for measurements. Spontaneously contracting, poor loaded cells or cells with spontaneous local Ca^{2+} release were excluded from evaluation. Fluorescence images (8-bit) were recorded using a 512 pixel scan line drawn along the longitudinal axis of the myocyte superfused with Tyrode's solution 2 (Table 10). Cytosolic and nuclear Ca^{2+} transients were recorded at 1 Hz stimulation at steady-state of the Ca^{2+} transient amplitude (baseline).

Table 10: Normal Tyrode's solution 2

Compound	Volume	Final concentration (mmol)
Normal Tyrode's solution 1 (Table 9)	250 ml	
$CaCl_2$ (1 molar stock solution)	250 µl	2

2.5 Image analysis

For steady-state Ca^{2+} transient (cytosolic, perinuclear and nuclear) analysis, data was converted to bitmap format by LSM Image Browser (Zeiss, Germany). Line scan images were segmented by the onset of the whole-line averaged Ca^{2+} transients and 8 to 9 consecutive transients were averaged using custom made algorithms coded in IDL (IDL 7.0, ITT Visual Information Solutions, Paris, France) as previously described [Heinzel et al., 2008, Lenaerts et al., 2009]. In each image cytoplasm, nucleus and perinuclear area were selected (Figure 14).

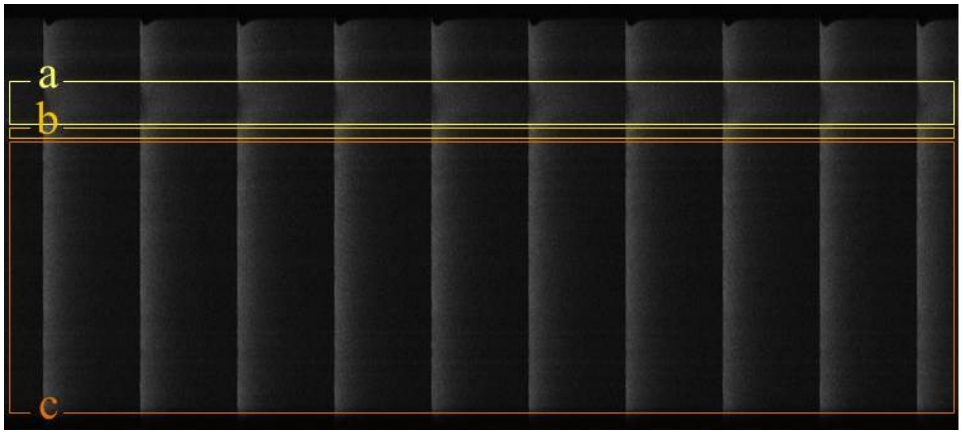

Figure 14: Original line scan image with regions of interest

Regions of interest: (a) nucleus, (b) perinuclear area and (c) cytoplasm.

Following parameters of Ca^{2+} transients were analyzed (Figure 15):

- Amplitude of the Ca^{2+} transient (F/F_0) within the subcellular compartment. The peak amplitude of the $[Ca^{2+}]_i$-dependent fluorescence (F) was divided by the averaged fluorescence during 30 ms interval before the onset of the Ca^{2+} transient (F_0).
- Time-to-peak (TTP), defined as the time from the stimulus until the peak amplitude of Ca^{2+} transient.
- Decay time, defined as the half-maximum relaxation time (RT50) and time to 90% relaxation (RT90).

Background fluorescence signal was subtracted from the F/F_0 value. Incompletely recorded transients (cut off at beginning or end) were deleted and excluded from further evaluation.

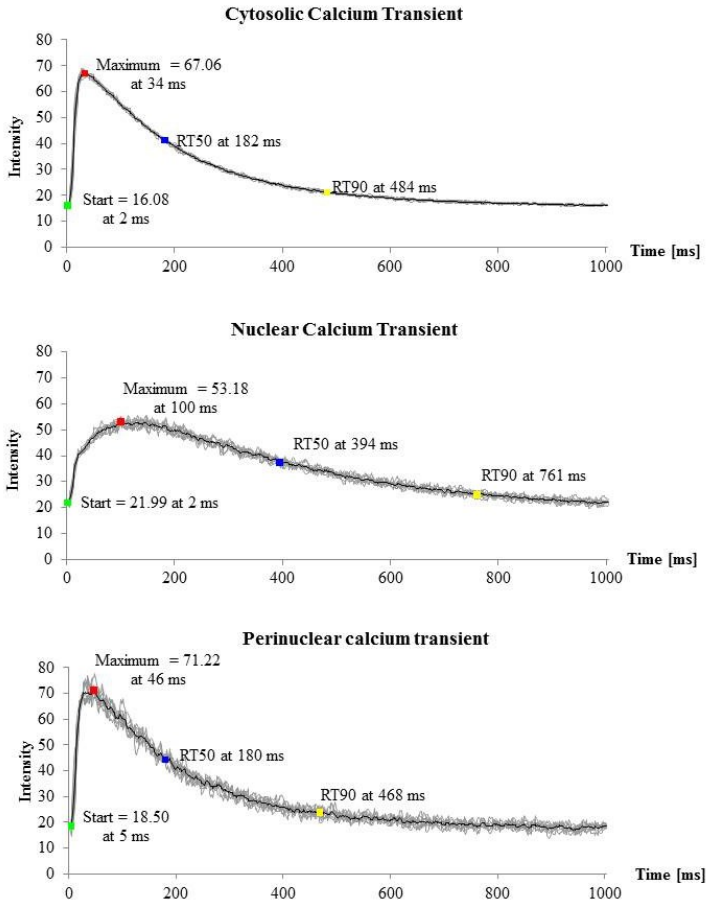

Figure 15: Calcium transient analysis

Indicated parameters were analyzed from cytoplasmic (top), nuclear (middle) and perinuclear (bottom) Ca^{2+} transients. Single Ca^{2+} transients (grey trace) were averaged (black trace) and the parameters were calculated. "Maximum" indicates time-to-peak (TTP), "RT50" represents half maximum relaxation time and "RT90" means 90% relaxation time.

2.6 Statistical Analysis

Data is given as mean ± standard error of the mean (S.E.M.), unless specified otherwise. Statistical analysis was performed with SPSS (IBM Corp. Released 2012. IBM SPSS Statistics for Windows, Version 21.0. Armonk, NY: IBM Corp.). Differences between groups were considered significant when $p<0.05$. For comparison of heart weight-to-body weight and heart weight-to-left tibia length ratio analysis of variance followed by Bonferroni post-hoc test were used. In order to account for non-normal distribution the Kruskal-Wallis Test with the Bonferroni-Holms method for *p* value adjustment was employed for comparison of Ca^{2+} transient amplitude and kinetics.

3 Results

3.1 Relative heart weight

Heart weight-to-body weight (HW/BW) and heart weight-to-tibia length (HW/TL) ratios were determined as parameters indicative of cardiac hypertrophy.

In WT-Sham mice, the HW/BW ratio was 8.02±0.48 mg/g, whereas the HW/TL ratio measured 9.96±0.66 mg/mm. Both parameters were significantly increased in WT-TAC mice and measured 10.83±0.53 mg/g and 13.58±0.59 mg/mm, respectively ($p<0.05$, Figure 16).

Similarly, HW/BW ratio significantly increased from 8.79±0.20 mg/g to 12.09±0.77 mg/g after 1 week TAC in RyR mice ($p<0.05$). HW/TL ratio increased from 11.79±0.44 mg/mm in Sham-operated animals to 14.78±0.38 mg/mm in RyR-TAC mice ($p<0.05$, Figure 16).

No significant differences were observed between Sham or TAC mice (WT vs. RyR) with respect to the HW/BW and HW/TL ratio.

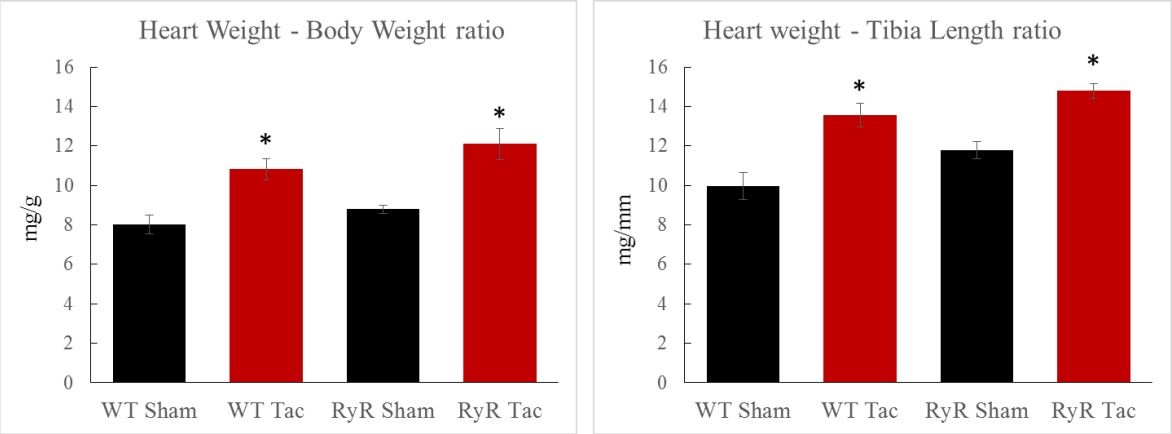

Figure 16: Increased HW/BW (left panel) and HW/TL (right panel) ratio in TAC groups

*$p<0.05$ versus respective sham

3.2 Cytoplasmic, nucleoplasmic and perinuclear Ca^{2+} transient amplitudes

At baseline, WT- and RyR-Sham mice had comparable cytoplasmic, nucleoplasmic and perinuclear Ca^{2+} transient amplitudes (Figures 17-19). One week after pressure overload, however, cytoplasmic Ca^{2+} transient amplitudes were significantly elevated in WT-TAC mice with respect to WT-Sham (from 3.31±0.16 to 4.03±0.17, $p<0.05$, Figure 17). On the contrary, a significant decrease in the cytosolic Ca^{2+} transient amplitudes was observed in RyR-TAC mice as compared to RyR-Sham (from 3.14±0.11 to 2.81±0.11) and WT-TAC mice (both $p<0.05$, Figure 17).

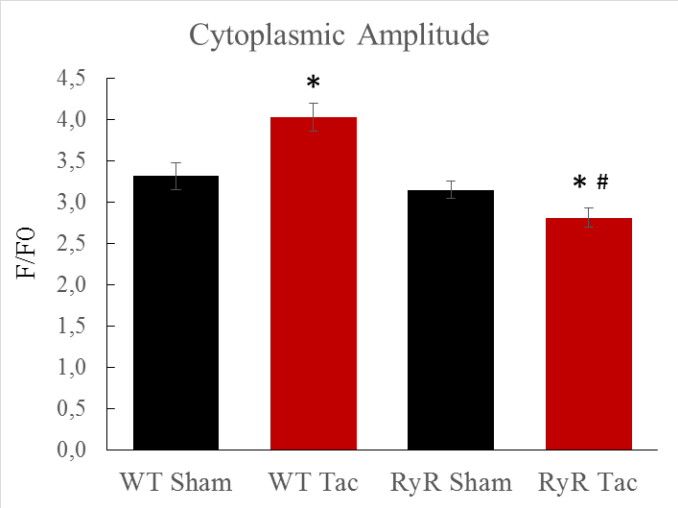

Figure 17: Mean cytoplasmic Ca^{2+} transient amplitudes
*$p<0.05$ versus respective sham, #$p<0.05$ versus WT-TAC

Nucleoplasmic Ca^{2+} transient amplitudes were elevated in WT mice after pressure-induced overload, but this did not reach statistical significance (from 2.13±0.06 to 2.42±0.10, $p=0.084$, Figure 18). On the other hand, RyR-TAC mice showed a significant decrease in the nucleoplasmic Ca^{2+} transient amplitudes compared to RyR-Sham (from 2.11±0.07 to 1.82±0.05 and WT-TAC cardiomyocytes (both $p<0.05$, Figure 18).

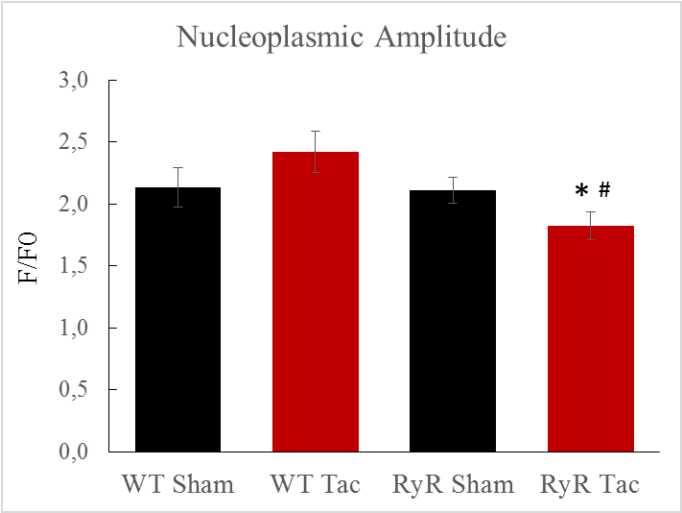

Figure 18: Mean nucleoplasmic Ca^{2+} transient amplitudes

*p<0.05 versus respective sham, $^{\#}p$<0.05 versus WT-TAC

TAC induced a significant increase in Ca^{2+} transient amplitudes from the perinuclear area in WT cardiomyocytes (from 2.96±0.12 to 3.82±0.17, p<0.05, Figure 19), whereas RyR-TAC cells had significantly decreased average Ca^{2+} transient amplitude in the perinuclear area compared to RyR-Sham (from 2.92±0.11 to 2.59±0.10) and WT-TAC myocytes (both p<0.05, Figure 19).

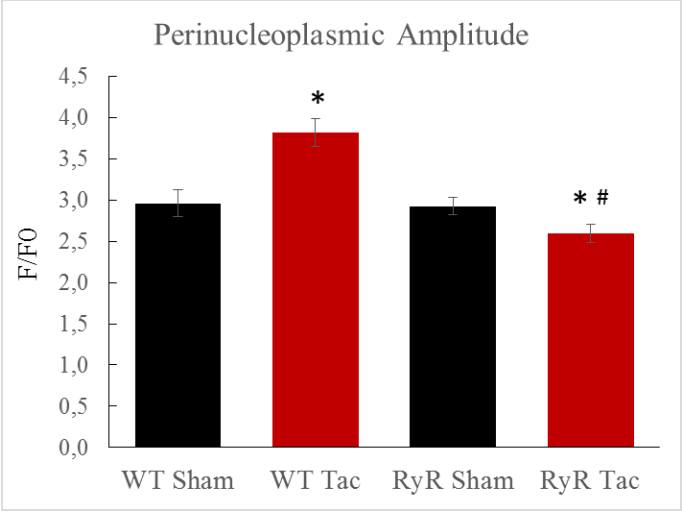

Figure 19: Mean perinucleoplasmic Ca^{2+} transient amplitudes

*p<0.05 versus respective sham, $^{\#}p$<0.05 versus WT-TAC

3.3 Ca^{2+} transient kinetics

3.3.1 Time-to-peak

No significant differences were found in cytoplasmic (Figure 20) and perinucleoplasmic (Figure 21) time-to-peak values of Ca^{2+} transients.

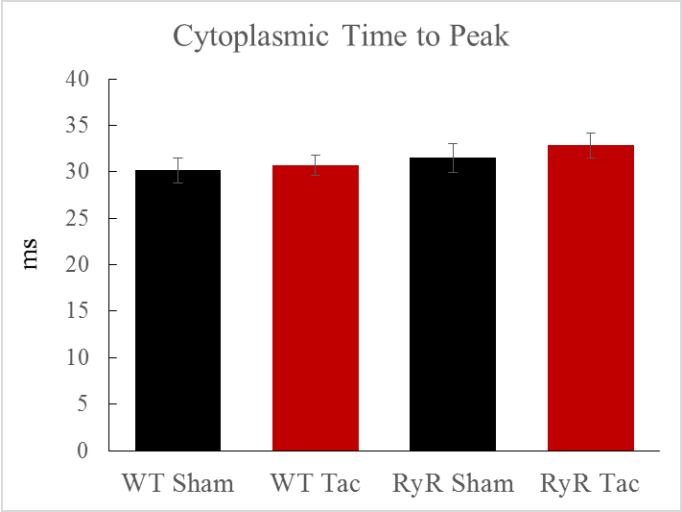

Figure 20: Time-to-peak of cytoplasmic Ca^{2+} transient

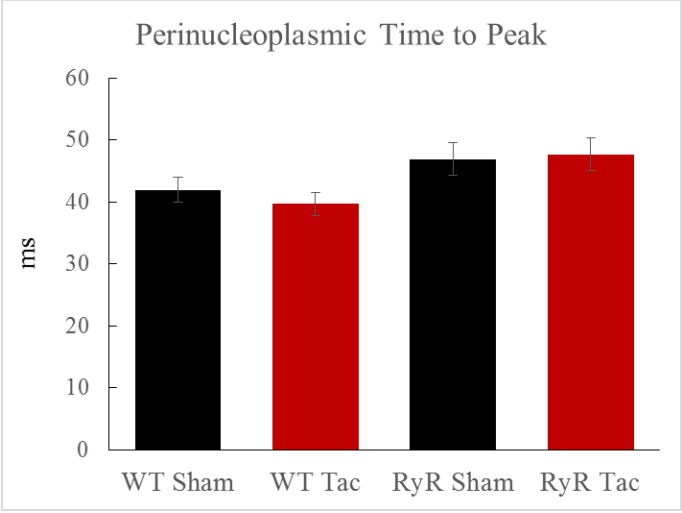

Figure 21: Time-to-peak of perinucleoplasmic Ca^{2+} transient

However, a marked increase of time-to-peak was observed in the nucleus from RyR-TAC cells as compared to RyR-Sham cardiomyocytes (140.18±5.44 ms versus 117.22±5.61 ms, $p<0.05$, respectively, Figure 22) and WT-TAC myocytes (114.37±5.40 ms, $p<0.05$ versus RyR-TAC). On the other hand, 1 week of pressure-induced overload did not significantly change the time-to-peak of nuclear Ca^{2+} amplitude in WT cardiomyocytes (Figure 22).

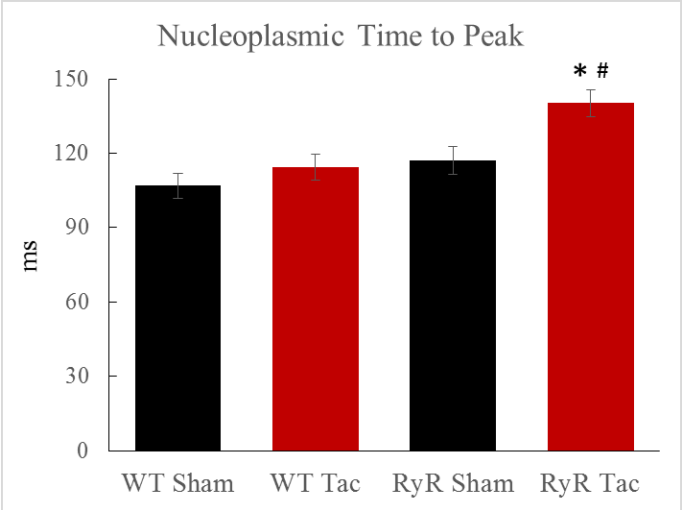

Figure 22: Time-to-peak of nuclear Ca^{2+} transient time

*$p<0.05$ versus respective sham, $^{\#}p<0.05$ versus WT-TAC

3.3.2 Decay time

At baseline, WT-Sham and RyR-Sham cardiomyocytes showed a similar Ca^{2+} transient amplitude decay (half-time of relaxation, RT_{50}) in the cytoplasm, nuclear and perinuclear area (Figures 23-25).

Similar cytoplasmic Ca^{2+} removal was observed in WT- and RyR-TAC cells compared to Sham-operated mice. However, RyR-TAC cells had significantly prolonged cytoplasmic RT50 compared to WT-TAC myocytes (245.44±6.31 ms versus 275.18±6.78 ms; $p<0.05$, Figure 23).

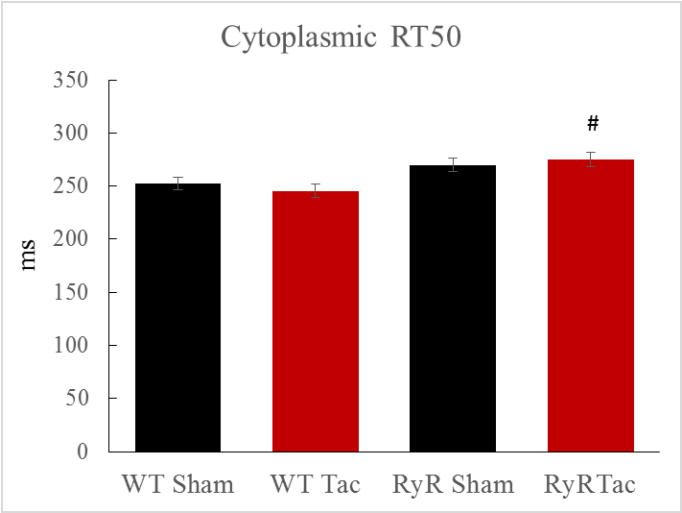

Figure 23: Cytoplasmic Ca^{2+} removal (RT50)

$^{\#}p<0.05$ versus WT-TAC

The same observation was made in the perinuclear area. While there was no significant difference between Sham and TAC animals, a significant prolongation was found between WT-TAC and RyR-TAC cardiomyocytes (243.23±6.98 ms versus 274.79± 7.47 ms, $p<0.05$, Figure 24).

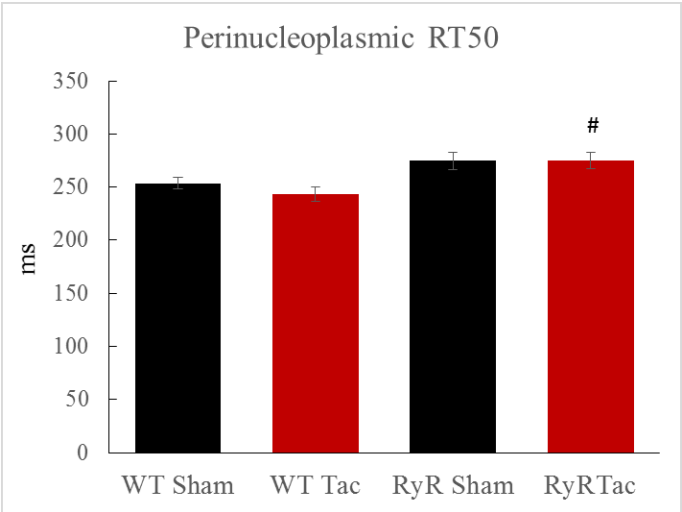

Figure 24: Perinuclear Ca^{2+} removal (RT50)

$^{\#}p<0.05$ versus WT-TAC

WT-Sham and WT-TAC cells had similar nuclear Ca^{2+} removal. On the other hand, RyR-TAC cells displayed marked prolongation nucleoplasmic Ca^{2+} decay (466.31±10.36 ms) to that of RyR control cells (498.90±9.09 ms, $p<0.05$, Figure 25). This prolongation was also significantly different from WT-TAC (446±11 ms, $p<0.05$, Figure 25).

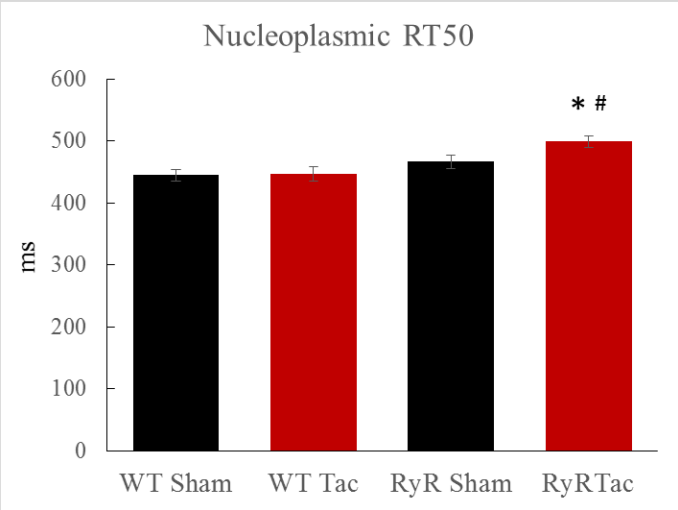

Figure 25: Nuclear Ca^{2+} removal (RT50)

*$p<0.05$ versus respective sham, $^{\#}p<0.05$ versus WT-TAC

Changes in RT90 were similar compared to RT50 in the cytoplasm, nuclear and perinuclear area between all groups (data not shown).

4 Discussion

The present study aimed to elucidate whether RyR2 dysfunction has an impact on the regulation of nuclear Ca^{2+} handling in response to pressure overload. We found that cardiomyocytes from Sham-operated mice showed similar cytoplasmic and nucleoplasmic Ca^{2+} transient amplitudes and kinetics. After 1 week TAC, however, the peak cytoplasmic Ca^{2+} transient amplitude was increased in WT cells, but nucleoplasmic Ca^{2+} transient amplitude and kinetics were normal. In contrast, RyR2-TAC cells had significantly smaller cytoplasmic and nucleoplasmic Ca^{2+} transient amplitudes as well as slower kinetics (time-to-peak and decay time) of nucleoplasmic Ca^{2+} transients.

4.1 Relative heart weight after TAC in RyR2 and WT mice

To confirm the development of hypertrophy after TAC, HW/BW and HW/TL ratio was determined. While HW/BW ratio is more common approach, HW/TL appears more robust and reliable measure of cardiac hypertrophy under conditions of larger variations in body weight of subjects [Yin et al., 1982]. In our study, however, both relative values showed the same degree of cardiac hypertrophy in WT and RyR2 mice. These results are in accordance with previously described hypertrophic changes in the TAC mouse model for pressure overload induced hypertrophy [Sedej et al., 2014].

4.2 Alterations of cytosolic, perinuclear and nuclear Ca^{2+} transients

4.2.1 Alterations in the peak Ca^{2+} amplitudes

The peak amplitudes of Ca^{2+} transients represent relative (non-calibrated) measures calculated from the (systolic) maximum of Ca^{2+} fluorescence signal divided by the (diastolic) baseline Ca^{2+} fluorescence level. Therefore, a decrease in the peak Ca^{2+} transient amplitude could result from a decrease in the maximum of Ca^{2+} fluorescence signal, but also from an increase in the baseline Ca^{2+} level. The same is true for an increase in the peak Ca^{2+} amplitude, which could mean a higher maximum Ca^{2+} value and/or a lower baseline Ca^{2+} level.

The cytosolic Ca^{2+} transient amplitudes of WT-TAC and RyR-TAC animals were found increased and decreased compared with the respective sham group. Increased Ca^{2+} amplitude in WT-TAC cells indicates increased contractility (positive inotropy) and an adaptive compensation of pressure overload. This finding is in accordance with a study by Mørk and colleagues, who described increased Ca^{2+} transients in early stage heart failure in a mouse infarct model [Mørk et al., 2007]. In contrast, RyR-TAC cardiomyocytes had decreased peak Ca^{2+} transient amplitude, suggesting decreased contractility (negative inotropy) and maladaptive compensation of pressure overload. This result could be explained by the increased SR Ca^{2+} leak in the mutated RyR animals that decreases SR Ca^{2+} content [Sedej et al., 2014].

While nuclear Ca^{2+} amplitudes were similar in WT-sham and WT-TAC animals, RyR-TAC cells showed a decrease in the nuclear Ca^{2+} amplitude compared to RyR-sham cardiomyocytes. Given the close proximity of the SR to the nucleus and increased RyR2-mediated SR Ca^{2+} release (SR Ca^{2+} leak) associated with the elevation of cytoplasmic baseline Ca^{2+}, we speculate that more Ca^{2+} diffuses into the nucleus through NPCs and elevates nuclear baseline Ca^{2+} concentration.

4.2.2 Alterations in the time-to-peak

Maladaptive T-tubule remodeling is an early event in the progression of hypertrophy towards heart failure. Loss of T-tubuli is associated with dysynchronous Ca^{2+} release and the prolonged time-to-peak [Wei et al., 2010]. However, we found no alterations in the perinuclear and cytoplasmic time-to-peak values, indicating no delay in the SR Ca^{2+} release due to T-tubuli remodeling 1 week after TAC.

Based on the previous finding that the time-to-peak correlates negatively with the number of nuclear invaginations in the progression of heart failure [Ljubojevic et al., 2014], the prolonged time-to-peak in nuclei of RyR-TAC cells may originate from an accelerated decrease of nuclear invaginations. As WT- and RyR-sham animals had no baseline differences in the time-to-peak, the combination of pressure overload (external trigger) and congenital RyR dysfunction is necessary to increase the time-to-peak in the nucleus.

4.2.3 Alterations in the decay time

Reduced removal of Ca^{2+} from the cytoplasm in RyR-TAC mice can be attributed to the depressed uptake of Ca^{2+} into the SR (due to reduced SERCA2a expression and activity), and the shift of Ca^{2+} removal from SERCA to NCX [Hasenfuss 1998]. Reduced SERCA expression has been found also in the nuclei of failing cardiomyocytes, which have reduced number of nuclear envelope invaginations [Ljubojevic et al., 2014]. Since nuclear Ca^{2+} has to diffuse through the inner nuclear membrane (out of the nucleus) in order to be removed, we hypothesize that these changes account for slower Ca^{2+} removal in the RyR-TAC nuclei (vs. RyR-sham group). In addition, RyR gain-of-function mutation enhanced these changes and led to delayed Ca^{2+} sequestration in the nucleus.

4.3 Future Perspective

This study showed that RyR2 dysfunction regulates nuclear Ca^{2+} in a mouse model of heart failure (induced by pressure overload). However, it remains to be shown that fixing the SR Ca^{2+} leak and stabilization of RyR2 restores nuclear Ca^{2+} handling. Moreover, it was shown that nuclear Ca^{2+} handling of failing cardiomyocytes is especially disrupted at higher frequencies [Ljubojevic et al., 2014]. Studies with higher frequencies are required to determine if higher pacing frequencies enhance changes in nuclear Ca^{2+} handling in mice carrying a gain-of-function RyR2 mutation. Finally, effects of the RyR2-mediated SR Ca^{2+} leak on genetic transcription and protein expression in the nucleus will need to be determined to improve our understanding of the role of RyR2 dysfunction in cardiac remodeling and the development of heart failure.

4.4 Conclusion and potential clinical relevance

The combination of acquired and congenital RyR2 dysfunction prolongs nuclear Ca^{2+} transients and reduces their amplitude in $RyR2^{R4496C+/-}$ hearts after pressure-induced overload. Our results suggest that RyR2-mediated Ca^{2+} changes in the nucleus may underlie altered gene expression (excitation-transcription coupling) and promote cardiac remodeling. Understanding the precise molecular regulation of aberrant SR Ca^{2+} leak signaling in cardiomyocytes from diseased hearts holds the promise to develop a new therapeutic approach against heart failure.

5 Bibliography

Ai, X., Curran, J. W., Shannon, T. R., Bers, D. M., & Pogwizd, S. M. (2005). Ca^{2+}/calmodulin-dependent protein kinase modulates cardiac ryanodine receptor phosphorylation and sarcoplasmic reticulum Ca^{2+} leak in heart failure. *Circulation Research, 97*(12), 1314-1322.

Bers, D. M. (2008). Calcium cycling and signaling in cardiac myocytes. *Annual Review of Physiology, 70*, 23-49.

Bers, D. M. (2002). Cardiac excitation-contraction coupling. *Nature, 415*(6868), 198-205.

Bers, D. M. (2004). Macromolecular complexes regulating cardiac ryanodine receptor function. *Journal of Molecular and Cellular Cardiology, 37*(2), 417-429.

Bers, D. M. (2008). Calcium cycling and signaling in cardiac myocytes. *Annual Review of Physiology, 70*, 23-49.

Beuckelmann, D. J., Nabauer, M., & Erdmann, E. (1992). Intracellular calcium handling in isolated ventricular myocytes from patients with terminal heart failure. *Circulation, 85*(3), 1046-1055.

Bootman, M. D., Fearnley, C., Smyrnias, I., MacDonald, F., & Roderick, H. L. (2009). An update on nuclear calcium signalling. *Journal of Cell Science, 122*(Pt 14), 2337-2350.

Bootman, M. D., Lipp, P., & Berridge, M. J. (2001). The organisation and functions of local Ca(2+) signals. *Journal of Cell Science, 114*(Pt 12), 2213-2222.

Braunwald, E. (2013). Heart failure. *JACC.Heart Failure, 1*(1), 1-20.

Carson, P., Anand, I., O'Connor, C., Jaski, B., Steinberg, J., Lwin, A., et al. (2005). Mode of death in advanced heart failure: The comparison of medical, pacing, and defibrillation therapies in heart failure (COMPANION) trial. *Journal of the American College of Cardiology, 46*(12), 2329-2334.

Cerrone, M., Colombi, B., Santoro, M., di Barletta, M. R., Scelsi, M., Villani, L., et al. (2005). Bidirectional ventricular tachycardia and fibrillation elicited in a knock-in mouse model carrier of a mutation in the cardiac ryanodine receptor. *Circulation Research, 96*(10), e77-82.

Dominguez-Rodriguez, A., Ruiz-Hurtado, G., Benitah, J. P., & Gomez, A. M. (2012). The other side of cardiac Ca(2+) signaling: Transcriptional control. *Frontiers in Physiology, 3*, 452.

Escobar, M., Cardenas, C., Colavita, K., Petrenko, N. B., & Franzini-Armstrong, C. (2011). Structural evidence for perinuclear calcium microdomains in cardiac myocytes. *Journal of Molecular and Cellular Cardiology, 50*(3), 451-459.

Fabiato, A. (1983). Calcium-induced release of calcium from the cardiac sarcoplasmic reticulum. *The American Journal of Physiology, 245*(1), C1-14.

Fearnley, C. J., Roderick, H. L., & Bootman, M. D. (2011). Calcium signaling in cardiac myocytes. *Cold Spring Harbor Perspectives in Biology, 3*(11), a004242.

Fischer, T. H., Maier, L. S., & Sossalla, S. (2013). The ryanodine receptor leak: How a tattered receptor plunges the failing heart into crisis. *Heart Failure Reviews, 18*(4), 475-483.

Franzini-Armstrong, C., Protasi, F., & Ramesh, V. (1999). Shape, size, and distribution of Ca(2+) release units and couplons in skeletal and cardiac muscles. *Biophysical Journal, 77*(3), 1528-1539.

Franzini-Armstrong, C., Protasi, F., & Tijskens, P. (2005). The assembly of calcium release units in cardiac muscle. *Annals of the New York Academy of Sciences, 1047*, 76-85.

Gomez, A. M., Valdivia, H. H., Cheng, H., Lederer, M. R., Santana, L. F., Cannell, M. B., et al. (1997). Defective excitation-contraction coupling in experimental cardiac hypertrophy and heart failure. *Science (New York, N.Y.), 276*(5313), 800-806.

Goody, R. S., & Holmes, K. C. (1983). Cross-bridges and the mechanism of muscle contraction. *Biochimica Et Biophysica Acta (BBA)-Reviews on Bioenergetics, 726*(1), 13-39.

Hasenfuss, G. (1998). Alterations of calcium-regulatory proteins in heart failure. *Cardiovascular Research, 37*(2), 279-289.

Hasenfuss, G., & Pieske, B. (2002). Calcium cycling in congestive heart failure. *Journal of Molecular and Cellular Cardiology, 34*(8), 951-969.

Hayashi, T., Martone, M. E., Yu, Z., Thor, A., Doi, M., Holst, M. J., et al. (2009). Three-dimensional electron microscopy reveals new details of membrane systems for Ca^{2+} signaling in the heart. *Journal of Cell Science, 122*(Pt 7), 1005-1013.

Heinzel, F. R., Bito, V., Biesmans, L., Wu, M., Detre, E., von Wegner, F., et al. (2008). Remodeling of T-tubules and reduced synchrony of Ca^{2+} release in myocytes from chronically ischemic myocardium. *Circulation Research, 102*(3), 338-346.

Hobai, I. A., & O'Rourke, B. (2001). Decreased sarcoplasmic reticulum calcium content is responsible for defective excitation-contraction coupling in canine heart failure. *Circulation, 103*(11), 1577-1584.

Hu, P., Zhang, D., Swenson, L., Chakrabarti, G., Abel, E. D., & Litwin, S. E. (2003). Minimally invasive aortic banding in mice: Effects of altered cardiomyocyte insulin signaling during pressure overload. *American Journal of Physiology Heart and Circulatory Physiology, 285*(3), H1261-9.

Kockskämper, J., Seidlmayer, L., Walther, S., Hellenkamp, K., Maier, L. S., & Pieske, B. (2008). Endothelin-1 enhances nuclear Ca^{2+} transients in atrial myocytes through ins(1,4,5)P3-dependent Ca^{2+} release from perinuclear Ca^{2+} stores. *Journal of Cell Science, 121*(Pt 2), 186-195.

Langer, G. A., & Peskoff, A. (1996). Calcium in the cardiac diadic cleft. implications for sodium-calcium exchange. *Annals of the New York Academy of Sciences, 779*, 408-416.

Lee, M. A., Dunn, R. C., Clapham, D. E., & Stehno-Bittel, L. (1998). Calcium regulation of nuclear pore permeability. *Cell Calcium, 23*(2-3), 91-101.

Lenaerts, I., Bito, V., Heinzel, F. R., Driesen, R. B., Holemans, P., D'hooge, J., et al. (2009). Ultrastructural and functional remodeling of the coupling between Ca^{2+} influx and sarcoplasmic reticulum Ca^{2+} release in right atrial myocytes from experimental persistent atrial fibrillation. *Circulation Research, 105*(9), 876-885.

Ljubojevic, S., & Bers, D. M. (2015). Nuclear calcium in cardiac myocytes. *Journal of Cardiovascular Pharmacology, 65*(3), 211-217.

Ljubojevic, S., Radulovic, S., Leitinger, G., Sedej, S., Sacherer, M., Holzer, M., et al. (2014). Early remodeling of perinuclear Ca^{2+} stores and nucleoplasmic Ca^{2+} signaling during the development of hypertrophy and heart failure. *Circulation, 130*(3), 244-255.

Ljubojevic, S., Walther, S., Asgarzoei, M., Sedej, S., Pieske, B., & Kockskamper, J. (2011). In situ calibration of nucleoplasmic versus cytoplasmic Ca^{2+} concentration in adult cardiomyocytes. *Biophysical Journal, 100*(10), 2356-2366.

Luo, M., & Anderson, M. E. (2013). Mechanisms of altered Ca^{2+} handling in heart failure. *Circulation Research, 113*(6), 690-708.

Lyon, A. R., MacLeod, K. T., Zhang, Y., Garcia, E., Kanda, G. K., Lab, M. J., et al. (2009). Loss of T-tubules and other changes to surface topography in ventricular myocytes from failing human and rat heart. *Proceedings of the National Academy of Sciences of the United States of America, 106*(16), 6854-6859.

Meyer, M., Schillinger, W., Pieske, B., Holubarsch, C., Heilmann, C., Posival, H., et al. (1995). Alterations of sarcoplasmic reticulum proteins in failing human dilated cardiomyopathy. *Circulation, 92*(4), 778-784.

Morimoto, S., O-Uchi, J., Kawai, M., Hoshina, T., Kusakari, Y., Komukai, K., et al. (2009). Protein kinase A-dependent phosphorylation of ryanodine receptors increases Ca^{2+} leak in mouse heart. *Biochemical and Biophysical Research Communications, 390*(1), 87-92.

Mørk, H. K., Sjaastad, I., Sande, J. B., Periasamy, M., Sejersted, O. M., & Louch, W. E. (2007). Increased cardiomyocyte function and Ca^{2+} transients in mice during early congestive heart failure. *Journal of Molecular and Cellular Cardiology, 43*(2), 177-186.

Muhlfeld, C., Schipke, J., Schmidt, A., Post, H., Pieske, B., & Sedej, S. (2013). Hypoinnervation is an early event in experimental myocardial remodelling induced by pressure overload. *Journal of Anatomy, 222*(6), 634-644.

Nakai, J., Imagawa, T., Hakamat, Y., Shigekawa, M., Takeshima, H., & Numa, S. (1990). Primary structure and functional expression from cDNA of the cardiac ryanodine receptor/calcium release channel. *FEBS Letters, 271*(1-2), 169-177.

Nattel, S., Maguy, A., Le Bouter, S., & Yeh, Y. H. (2007). Arrhythmogenic ion-channel remodeling in the heart: Heart failure, myocardial infarction, and atrial fibrillation. *Physiological Reviews, 87*(2), 425-456.

Neumann, J., Eschenhagen, T., Jones, L. R., Linck, B., Schmitz, W., Scholz, H., et al. (1997). Increased expression of cardiac phosphatases in patients with end-stage heart failure. *Journal of Molecular and Cellular Cardiology, 29*(1), 265-272.

O'Connell, T. D., Ni, Y. G., Lin, K., Han, H., & Yan, Z. (2003). Isolation and culture of adult mouse cardiac myocytes for signaling studies. *AfCS Research Reports, 1*(5), 1-9.

Otsu, K., Willard, H. F., Khanna, V. K., Zorzato, F., Green, N. M., & MacLennan, D. H. (1990). Molecular cloning of cDNA encoding the Ca^{2+} release channel (ryanodine receptor) of rabbit cardiac muscle sarcoplasmic reticulum. *The Journal of Biological Chemistry, 265*(23), 13472-13483.

Paddock, S. W. (2000). Principles and practices of laser scanning confocal microscopy. *Molecular Biotechnology, 16*(2), 127-149.

Pessah, I. N., Waterhouse, A. L., & Casida, J. E. (1985). The calcium-ryanodine receptor complex of skeletal and cardiac muscle. *Biochemical and Biophysical Research Communications, 128*(1), 449-456.

Piacentino, V.,3rd, Weber, C. R., Chen, X., Weisser-Thomas, J., Margulies, K. B., Bers, D. M., et al. (2003). Cellular basis of abnormal calcium transients of failing human ventricular myocytes. *Circulation Research, 92*(6), 651-658.

Pieske, B., Maier, L. S., Piacentino, V.,3rd, Weisser, J., Hasenfuss, G., & Houser, S. (2002). Rate dependence of [na+]i and contractility in nonfailing and failing human myocardium. *Circulation, 106*(4), 447-453.

Reiken, S., Gaburjakova, M., Guatimosim, S., Gomez, A. M., D'Armiento, J., Burkhoff, D., et al. (2003). Protein kinase A phosphorylation of the cardiac calcium release channel (ryanodine receptor) in normal and failing hearts. role of phosphatases and response to isoproterenol. *The Journal of Biological Chemistry, 278*(1), 444-453.

Sedej, S., Heinzel, F. R., Walther, S., Dybkova, N., Wakula, P., Groborz, J., et al. (2010). Na+-dependent SR Ca^{2+} overload induces arrhythmogenic events in mouse cardiomyocytes with a human CPVT mutation. *Cardiovascular Research, 87*(1), 50-59.

Sedej, S., Schmidt, A., Denegri, M., Walther, S., Matovina, M., Arnstein, G., et al. (2014). Subclinical abnormalities in sarcoplasmic reticulum Ca(2+) release promote eccentric myocardial remodeling and pump failure death in response to pressure overload. *Journal of the American College of Cardiology, 63*(15), 1569-1579.

Shigekawa, M., & Iwamoto, T. (2001). Cardiac Ca(+)-Ca(2+) exchange: Molecular and pharmacological aspects. *Circulation Research, 88*(9), 864-876.

Shotton, D. M. (1989). Confocal scanning optical microscopy and its applications for biological specimens. *Journal of Cell Science, 94*(2), 175-206.

Signore, S., Sorrentino, A., Ferreira-Martins, J., Kannappan, R., Shafaie, M., Del Ben, F., et al. (2013). Inositol 1, 4, 5-trisphosphate receptors and human left ventricular myocytes. *Circulation, 128*(12), 1286-1297.

Soeller, C., & Cannell, M. B. (1999). Examination of the transverse tubular system in living cardiac rat myocytes by 2-photon microscopy and digital image-processing techniques. *Circulation Research, 84*(3), 266-275.

Song, L. S., Sobie, E. A., McCulle, S., Lederer, W. J., Balke, C. W., & Cheng, H. (2006). Orphaned ryanodine receptors in the failing heart. *Proceedings of the National Academy of Sciences of the United States of America, 103*(11), 4305-4310.

Tarazon, E., Rivera, M., Rosello-Lleti, E., Molina-Navarro, M. M., Sanchez-Lazaro, I. J., Espana, F., et al. (2012). Heart failure induces significant changes in nuclear pore complex of human cardiomyocytes. *PloS One, 7*(11), e48957.

Toischer, K., Rokita, A. G., Unsold, B., Zhu, W., Kararigas, G., Sossalla, S., et al. (2010). Differential cardiac remodeling in preload versus afterload. *Circulation, 122*(10), 993-1003.

van Oort, R. J., Respress, J. L., Li, N., Reynolds, C., De Almeida, A. C., Skapura, D. G., et al. (2010). Accelerated development of pressure overload-induced cardiac hypertrophy and dysfunction in an RyR2-R176Q knockin mouse model. *Hypertension, 55*(4), 932-938.

Wei, S., Guo, A., Chen, B., Kutschke, W., Xie, Y. P., Zimmerman, K., et al. (2010). T-tubule remodeling during transition from hypertrophy to heart failure. *Circulation Research, 107*(4), 520-531.

Wu, X., & Bers, D. M. (2006). Sarcoplasmic reticulum and nuclear envelope are one highly interconnected Ca^{2+} store throughout cardiac myocyte. *Circulation Research, 99*(3), 283-291.

Wu, X., Zhang, T., Bossuyt, J., Li, X., McKinsey, T. A., Dedman, J. R., et al. (2006). Local InsP3-dependent perinuclear Ca^{2+} signaling in cardiac myocyte excitation-transcription coupling. *The Journal of Clinical Investigation, 116*(3), 675-682.

Yin, F. C., Spurgeon, H. A., Rakusan, K., Weisfeldt, M. L., & Lakatta, E. G. (1982). Use of tibial length to quantify cardiac hypertrophy: Application in the aging rat. *The American Journal of Physiology, 243*(6), H941-7.